# Global dynamics and asymptotics for monomial scalar field potentials and perfect fluids

Artur Alho,[1][*] Juliette Hell[2][†] and Claes Uggla[3][‡]

[1]*Center for Mathematical Analysis, Geometry and Dynamical Systems,*

*Instituto Superior Técnico, Universidade de Lisboa,*

*Av. Rovisco Pais, 1049-001 Lisboa, Portugal.*

[2]*Freie Universität Berlin, Institut für Mathematik,*

*Arnimallee 3D - 14195 Berlin, Germany.*

[3]*Department of Physics, University of Karlstad,*

*S-65188 Karlstad, Sweden.*

## Abstract

We consider a minimally coupled scalar field with a monomial potential and a perfect fluid in flat FLRW cosmology. We apply local and global dynamical systems techniques to a new three-dimensional dynamical systems reformulation of the field equations on a compact state space. This leads to a visual global description of the solution space and asymptotic behavior. At late times we employ averaging techniques to prove statements about how the relationship between the equation of state of the fluid and the monomial exponent of the scalar field affects asymptotic source dominance and asymptotic manifest self-similarity breaking. We also situate the 'attractor' solution in the three-dimensional state space and show that it corresponds to the one-dimensional unstable center manifold of a de Sitter fixed point, located on an unphysical boundary associated with the dynamics at early times. By deriving a center manifold expansion we obtain approximate expressions for the attractor solution. We subsequently improve the accuracy and range of the approximation by means of Padé approximants and compare with the slow-roll approximation.

[*]Electronic address:`aalho@math.ist.utl.pt`

[†]Electronic address:`blanca@math.fu-berlin.de`

[‡]Electronic address:`claes.uggla@kau.se`

1

# 1  Introduction

The present paper investigates general relativistic flat Friedmann-Lemaître-Robertson-Walker (FLRW) models with a minimally coupled scalar field with a monomial potential, $V(\phi) = \frac{1}{2n}(\lambda\phi)^{2n}$ ($\lambda > 0$, $n = 1, 2, 3, \dots$), and a perfect fluid. The perfect fluid is assumed to obey a linear equation of state, $p_m = (\gamma_m - 1)\rho_m$, where $p_m$ and $\rho_m \geq 0$ are the pressure and the energy density, respectively. The adiabatic index is assumed to satisfy $0 < \gamma_m < 2$, where $\gamma_m = 1$ corresponds to dust and $\gamma_m = 4/3$ to radiation. When $\gamma_m = 2/3$ the matter term $\rho_m$ can be reinterpreted as $-\frac{1}{2}{}^3R$, where ${}^3R$ is the spatial 3-curvature of the open FLRW model, i.e., $\gamma_m = 2/3$ leads to equations that are the same as those for a scalar field in open FLRW cosmology. The case $\gamma_m = 0$ corresponds to a matter content described by a cosmological constant, i.e., $\rho_m = \Lambda$, while $\gamma_m = 2$ describes a stiff perfect fluid; both cases are associated with significant bifurcations, and we therefore refrain from discussing them.

The Einstein and matter field equations for these models are given by

$$3H^2 = \tfrac{1}{2}\dot{\phi}^2 + \frac{1}{2n}(\lambda\phi)^{2n} + \rho_m = \rho_\phi + \rho_m, \tag{1a}$$

$$\dot{H} = -\tfrac{1}{2}\left(\dot{\phi}^2 + \gamma_m\rho_m\right), \tag{1b}$$

$$0 = \ddot{\phi} + 3H\dot{\phi} + \lambda^{2n}\phi^{2n-1}, \tag{1c}$$

$$\dot{\rho}_m = -3H\gamma_m\rho_m. \tag{1d}$$

Here an overdot signifies the derivative with respect to synchronous proper time, $t$; $H$ is the Hubble variable, which is given by $H = \dot{a}/a$, where $a(t)$ is the cosmological scale factor, and throughout we assume an expanding Universe, i.e. $H > 0$, where $H$ is related to the expansion $\theta$ according to $H = \theta/3$. We use (reduced Planck) units such that $c = 1 = 8\pi G$, where $c$ is the speed of light and $G$ is the gravitational constant (in the inflationary literature the gravitational constant $G$ is often replaced by the Planck mass, $G = 1/m_{\mathrm{Pl}}^2$).

Heuristically eq. (1c) can be viewed as an equation for an anharmonic oscillator with a friction term $3H\dot{\phi}$. This suggests that $(\dot{\phi}, \phi) \to (0, 0)$ toward the future in an oscillatory manner, which is indeed correct. This qualitative picture, however, does not show how this comes about in a quantitative way, nor how the fluid affects the situation via its influence on $H$. Running the time backwards allows one to heuristically interpret $3H\dot{\phi}$ as an energy input, which suggests that the scalar field oscillates with increasing amplitude toward the past, but this picture breaks down in the limit $H \to \infty$. Even though this is beyond the Planck regime, this limit is also needed in order to describe the classical behavior at early times after the Planck epoch. Furthermore, eq. (1d) yields that

$$\rho_m = \rho_0(a/a_0)^{-3\gamma_m}, \tag{2}$$

where $\rho_0$ an $a_0$ are constants, and hence $\rho \to 0$ at late times while $\rho \to \infty$ at early times.

Note that the above qualitative considerations say nothing about how e.g.

$$r = \frac{\rho_\phi}{\rho_m} \tag{3}$$

behaves asymptotically, i.e., if the model is fluid or scalar field dominated, or neither, asymptotically. Nor does the above say anything about the role of the so-called attractor solution in a global solution space setting.

This exemplifies that there is a need for a more careful examination, which is illustrated by some previous heuristic considerations for a scalar field with a monomial potential by e.g. Turner [1] and Mukhanov [2] p. 242, which in turn inspired the rigorous work by Rendall [3]; in addition de la Macorra and Piccinelli introduced a new heuristic approach to study dynamics at late times for a scalar field with a monomial potential and a perfect fluid [4]; rigorous work in this context was also obtained for the special case $n = 1$ by Giambo and Miritzis [5].[1] Nevertheless, this still leaves room for improvements and extensions, and, as will be shown in this paper, it is possible to shed light on interesting previously neglected physical and mathematical aspects.

The main purpose of this paper in, primarily, mathematical cosmology is two-fold: Firstly, to obtain a global visual picture of the solutions space, thus, e.g., situating the so-called attractor solution in a global solution space context. Secondly, to prove issues concerning asymptotical behavior at late and early times. This includes introducing averaging techniques to determine late time behavior, generalizing and simplifying earlier proofs in the literature, and using center manifold theory to rigorously derive approximations for the attractor solution at early times, as well as clarifying the physically important issue of asymptotic self-similarity.

The outline of the paper is as follows. In the next section we introduce our new three-dimensional dynamical systems reformulation of the field equations on a relatively compact state space. We also present two other complementary dynamical systems formulations of the field equations, which allow us to effectively obtain approximations for the attractor solution. In Section 3 we apply global and local dynamical systems techniques to obtain a complete and illustrative picture of the solution space and its properties, including asymptotics. In particular, we introduce averaging techniques in our global dynamical systems setting, which allows us to prove the following theorem:

**Theorem 1.1.**

(i) If $\gamma_m - \frac{2n}{n+1} > 0$, then $r = \rho_\phi/\rho_m \to \infty$ for all solutions with $\rho_\phi\rho_m > 0$, which implies that the solutions are future *asymptotically scalar field dominated*.

(ii) If $\gamma_m - \frac{2n}{n+1} < 0$, then $r = \rho_\phi/\rho_m \to 0$ for all solutions with $\rho_\phi\rho_m > 0$, and thus the solutions in this case are future *asymptotically perfect fluid dominated*.

---

[1]Some further examples of references that describe minimally coupled scalar field cosmology in dynamical systems settings are [6, 7, 8], with additional references therein.

(iii) If $\gamma_m - \frac{2n}{n+1} = 0$, then $r = \rho_\phi/\rho_m \to$ const. when $\rho_\phi \rho_m > 0$, and there is thus no future scalar field or perfect fluid dominance.

It should be pointed out that similar conclusions have been reached heuristically with quite different arguments in e.g. [4]. Furthermore, Giambo and Miritzis gave a proof for $n = 1$ for the cases (i) and (ii) in [5] (in the case of general relativity). However, apart from that our proof rigorously generalizes previous results, our method can, in principle, be modified to treat even more general situations. Moreover, we tie our results to the global dynamical systems picture and discuss their physical implications, e.g., situating them in the context of future manifest asymptotic self-similarity breaking. In Section 4 we focus on the attractor solution, where we introduce and compare several approximation schemes, such as center manifold and slow-roll based expansions and Padé approximants, in order to describe it quantitatively. Finally, Section 5 contains some general remarks, e.g. about the de Sitter solution on the unphysical boundary of the state space.

# 2   Dynamical systems formulations

## 2.1   Global dynamical systems

Our main global (i.e. compact) dynamical systems formulation is based on the dependent variables $T, X, \Sigma_\dagger$, which are defined as follows:

$$(T, X, \Sigma_\dagger) = \left( \frac{c}{c + H^{1/n}}, \frac{\lambda\phi}{(6nH^2)^{1/2n}}, \frac{\dot{\phi}}{\sqrt{6}H} \right), \tag{4a}$$

$$(H, \phi, \dot{\phi}) = \left( c^n \tilde{T}^{-n}, \sqrt{6}\tilde{T}^{-1}X, \sqrt{6}c^n\tilde{T}^{-n}\Sigma_\dagger \right), \tag{4b}$$

where

$$\tilde{T} = \frac{T}{1 - T}, \qquad c = \left( \frac{6^{n-1}}{n} \right)^{\frac{1}{2n}} \lambda. \tag{4c}$$

In addition it is of interest to define

$$\Omega_\phi = \frac{\rho_\phi}{3H^2} = \Sigma_\dagger^2 + X^{2n}, \qquad \Omega_m = \frac{\rho_m}{3H^2}. \tag{5}$$

To introduce a new suitable time variable we note the following: At early times it is natural to use a Hubble-normalized time variable $\tau$ defined by $d\tau/dt = H$, due to that the expansion $\theta = 3H$ provides a natural variable scale when $\theta \to \infty$ via the Raychaudhuri equation, as further discussed in e.g. [9], and references therein (in an inflationary context $\tau$ is often interpreted as the number of $e$-folds $N$). At late times the square root of the second derivative of the potential, $\phi^{n-1}$ (for simplicity we here incorporate $\lambda$ into $\phi$), provides a natural variable (mass) scale. Due to the

Gauss constraint (1a), which relates a scale given in $\phi$ to one given in $H$ according to $\phi \sim H^{1/n}$, this scale can be expressed in terms $H$ according to $H^{1-1/n}$ which leads to a dimensionless time variable $\check{\tau}$ defined by $d\check{\tau}/dt = \text{constant} \cdot H^{1-1/n}$, where the constant have the same dimension as $H^{1/n}$. To incorporate these features in a global dynamical systems setting we introduce a new time variable $\bar{\tau}$ that interpolates between these two regimes,

$$\frac{d\bar{\tau}}{dt} = H(1-T)^{-1}, \tag{6}$$

where $d\bar{\tau}/dt \to H$, $cH^{1-1/n}$ when $\bar{\tau} \to -\infty$ and $\bar{\tau} \to +\infty$, respectively.

The above leads to the following three-dimensional dynamical system for $(T, \Sigma_\dagger, X)$:[2]

$$\frac{dT}{d\bar{\tau}} = \frac{1}{n}T(1-T)^2(1+q), \tag{7a}$$

$$\frac{d\Sigma_\dagger}{d\bar{\tau}} = -(1-T)(2-q)\Sigma_\dagger - nTX^{2n-1}, \tag{7b}$$

$$\frac{dX}{d\bar{\tau}} = \frac{1}{n}(1-T)(1+q)X + T\Sigma_\dagger, \tag{7c}$$

where the deceleration parameter, $q$, defined via $\dot{H} = -(1+q)H^2$, is given by

$$q = -1 + \frac{3}{2}\left(\gamma_\phi\Omega_\phi + \gamma_m\Omega_m\right) = -1 + 3\Sigma_\dagger^2 + \frac{3}{2}\gamma_m\Omega_m, \tag{8}$$

where

$$\Omega_\phi = \Sigma_\dagger^2 + X^{2n}, \qquad \Omega_m = 1 - \Sigma_\dagger^2 - X^{2n} = 1 - \Omega_\phi \geq 0, \tag{9}$$

where the last equation follows from the Gauss constraint (1a), while the inequality is due to $\rho_m \geq 0$. Above we have also introduced an effective equation of state parameter $\gamma_\phi$ for the scalar field which is defined according to

$$\gamma_\phi = 1 + \frac{p_\phi}{\rho_\phi} = 1 + \frac{\frac{1}{2}\dot{\phi}^2 - \frac{1}{2n}(\lambda\phi)^{2n}}{\frac{1}{2}\dot{\phi}^2 + \frac{1}{2n}(\lambda\phi)^{2n}} = \frac{\dot{\phi}^2}{\frac{1}{2}\dot{\phi}^2 + \frac{1}{2n}(\lambda\phi)^{2n}}. \tag{10}$$

From the above relations it follows that $-1 \leq q \leq 2$. In addition it is of interest to give the following auxiliary evolution equation for $\Omega_\phi$:

$$\frac{d\Omega_\phi}{d\bar{\tau}} = 3(1-T)(\gamma_m - \gamma_\phi)\Omega_\phi\Omega_m, \tag{11}$$

---

[2]The variable $\Sigma_\dagger$ has been used ubiquitously in the scalar field literature (often denoted by $x$), while $X$ was used in [10] where it was denoted by $y$, however, as far as we know, the variable $T$ and the independent variable $\bar{\tau}$ are new. The reason for the name $\Sigma_\dagger$ is that mathematically this variable plays a role that is reminiscent to that of Hubble-normalized shear, which is usually denominated by $\Sigma$ in anisotropic cosmology, for a number of situations (the subscript $\dagger$ follows the notation in [11]). Thus the present nomenclature is designed to pave the way for eventually situating the present problem in a broader context than isotropic scalar field cosmology.

where

$$\gamma_\phi \Omega_\phi = 2\Sigma_\dagger^2. \tag{12}$$

The state space $\mathbf{S}$ associated with eq. (7) is given by a finite (when $n > 1$ deformed) cylinder described by the invariant pure *scalar field boundary subset*, $\Omega_m = 0$ (i.e. $\rho_m = 0$), and thus $\Omega_\phi = 1$, which we denote by $\mathbf{S}|_{\Omega_m=0}$, and $0 < T < 1$. From now on, we analytically extend $\mathbf{S}$ to the state space $\bar{\mathbf{S}}$ by including the unphysical invariant submanifold boundaries $T = 0$ and $T = 1$. Although these boundaries are unphysical, we stress that it is essential to include them since they describe the past and future asymptotic states, respectively, of all physical solutions.

Note that $\Omega_\phi = 0$ (i.e. $\Sigma_\dagger = 0 = X$) and hence $\Omega_m = 1$ is an interior invariant subset, $\mathbf{S}|_{\Omega_\phi=0}$, which is just a straight line in the center of the cylinder, describing the flat FLRW perfect fluid model without a scalar field (this solution appears as a straight line in the present state space due to that it is a self-similar solution, where $T$ describes the temporal change in the dimensional variable $H$). Note also that the dynamical system (7) is invariant under the discrete symmetry $(X, \Sigma_\dagger) \to -(X, \Sigma_\dagger)$, leading to a double representation of the physical solutions when $\Omega_m > 0$, which is a consequence of that the potential is invariant when $\phi \to -\phi$.[3]

To describe the dynamics on the scalar field boundary $\bar{\mathbf{S}}|_{\Omega_m=0}$, where $\Omega_\phi = 1$, it is useful to introduce a complementary global formulation, which is based on the following transformation of $\Sigma_\dagger$ and $X$:

$$\Sigma_\dagger = F(\theta) \sin \theta, \qquad X = \cos \theta, \qquad F(\theta) = \sqrt{\frac{1 - \cos^{2n} \theta}{1 - \cos^2 \theta}}. \tag{13}$$

This leads to the following regular *unconstrained* two-dimensional dynamical system:

$$\frac{dT}{d\bar{\tau}} = \frac{3}{n} T(1 - T)^2 (1 - \cos^{2n} \theta), \tag{14a}$$

$$\frac{d\theta}{d\bar{\tau}} = -TF(\theta) - \frac{3}{2n}(1 - T)F^2(\theta) \sin 2\theta. \tag{14b}$$

In this case the deceleration parameter $q$ is given by

$$q = 2 - 3 \cos^{2n} \theta. \tag{15}$$

The system (14) constitutes a generalization of the system used in [12]. Note that for $n > 1$ the present $\theta$ variable is not the same $\theta$ as that in [3], which in turn was based on the variables used in [13].

---

[3]The system (7) is differentiable for non-integer $n$ when $n > 1$, where the differentiability depends on $n$, describing problems with potentials $V = \frac{1}{2n}(\lambda|\phi|)^{2n}$, where $X$ is to be replaced with $|X|$ in (7).

## 2.2   Complementary non-bounded dynamical systems

We here introduce two complementary dynamical systems on unbounded state spaces that are useful for describing the dynamics at early times. The first system is based on the dependent variables $\tilde{T}, X, \Sigma_\dagger$ and the independent variable $\tau$, where we recall that $\tilde{T}$ and $\tau$ are defined by

$$\tilde{T} = \frac{T}{1 - T} = cH^{-1/n}, \qquad \frac{d\tau}{dt} = H, \tag{16}$$

where $\tau$ can be viewed as the number of $e$-folds $N$, i.e., $\tau = N$. This leads to the dynamical system:

$$\frac{d\tilde{T}}{d\tau} = \frac{1}{n}\tilde{T}(1 + q), \tag{17a}$$

$$\frac{d\Sigma_\dagger}{d\tau} = -(2 - q)\Sigma_\dagger - n\tilde{T}X^{2n-1}, \tag{17b}$$

$$\frac{dX}{d\tau} = \frac{1}{n}(1 + q)X + \tilde{T}\Sigma_\dagger, \tag{17c}$$

where $q$ is still given by (8), (9).[4] It is also useful to consider auxiliary equations for $\Omega_\phi$ and $r = \rho_\phi/\rho_m = \Omega_\phi/\Omega_m$:

$$\frac{d\Omega_\phi}{d\tau} = 3(\gamma_m - \gamma_\phi)\Omega_\phi\Omega_m, \tag{18a}$$

$$\frac{dr}{d\tau} = 3(\gamma_m - \gamma_\phi)r. \tag{18b}$$

The second complementary dynamical system concerns the dynamics on the scalar field boundary $\Omega_m = 0$. Expressed in terms of $\tilde{T}$ and $\tau$ the unconstrained system (14) takes the form:

$$\frac{d\tilde{T}}{d\tau} = \frac{3}{n}\tilde{T}(1 - \cos^{2n}\theta), \tag{19a}$$

$$\frac{d\theta}{d\tau} = -\tilde{T}F(\theta) - \frac{3}{2n}F^2(\theta)\sin 2\theta. \tag{19b}$$

Note that the above systems share the same equations as the previous ones with bounded state spaces on the invariant boundary subset $\tilde{T} = 0 = T$.

# 3   Global dynamical systems analysis

It follows from (7) that

$$\left.\frac{dT}{d\bar{\tau}}\right|_{1+q=0} = 0, \qquad \left.\frac{d^2T}{d\bar{\tau}^2}\right|_{1+q=0} = 0, \qquad \left.\frac{d^3T}{d\bar{\tau}^3}\right|_{1+q=0} = 6nT^3(1 - T)^2, \tag{20}$$

---

[4]In the special case $\Omega_m = 0$ and $n = 2$ this system coincides with eq. (16) in [14]; incidentally, this model was also the example discussed by Linde in his paper "Chaotic inflation" [15].

on **S** (note that since we have assumed that $\gamma_m > 0$ it follows from eq. (8) that $q+1 = 0$ only when $\Omega_m = 0$ and $\gamma_\phi = 0$). Due to that $q+1 \geq 0$, it follows from (7a) and (20) that $T$ is a monotonically increasing function on **S** (although eq. (20) shows that solutions on the scalar field boundary have inflection points when $1+q = 0$) and hence $T$ can be viewed as a time variable if one is so inclined. As a consequence all orbits (i.e. solution trajectories) in **S** originate from the invariant subset boundary $T = 0$, which is associated with the asymptotic (classical) initial state, and end at the invariant subset boundary $T = 1$, which corresponds to the asymptotic future, and therefore all fixed points are located at $T = 0$ and $T = 1$.[5] It also follows from the monotonicity of $T$ that the past (future) attractor resides on $T = 0$ ($T = 1$).

The equations on the subset $T = 0$ (or, equivalently $\tilde{T} = 0$) are given by

$$\frac{d\Sigma_\dagger}{d\bar{\tau}} = -(2 - q)\Sigma_\dagger, \tag{21a}$$

$$\frac{dX}{d\bar{\tau}} = \frac{1}{n}(1 + q)X, \tag{21b}$$

as follows from (7), or, equivalently (17) (with $\bar{\tau}$ replaced with $\tau$), where $q$ is given by (8) and (9). It follows that the state space on $T = 0$ is divided into four sectors defined by the invariant subsets $\Sigma_\dagger = 0$ and $X = 0$. The intersection of these subsets with $\Omega_m = 0$ and with each other yield five fixed points on $T = 0$:

$$\begin{aligned} \text{M}_\pm: \quad & X = 0, \quad & \Sigma_\dagger = \pm 1, & \tag{22a}\\ \text{dS}_\pm: \quad & X = \pm 1, \quad & \Sigma_\dagger = 0, & \tag{22b}\\ \text{FL}_0: \quad & X = 0, \quad & \Sigma_\dagger = 0, & \tag{22c} \end{aligned}$$

where $\text{M}_\pm$ are two equivalent fixed points for which $\Omega_m = 0$ and $q = 2$ (and $\gamma_\phi = 2$), i.e., they are associated with a massless scalar field state, while the two equivalent fixed points $\text{dS}_\pm$, for which $\Omega_m = 0$ and $q = -1$ (and $\gamma_\phi = 0$) correspond to a de Sitter state.[6] The fixed point $\text{FL}_0$ gives $\Omega_m = 1$ and $q = \frac{1}{2}(3\gamma_m - 2)$ and corresponds to the flat perfect fluid Friedman model.

As shown below, the two fixed points $\text{M}_\pm$ are sources on $\bar{\textbf{S}}$; the fixed points $\text{dS}_\pm$ are sinks *on* $T = 0$, but they also have one zero eigenvalue that corresponds to a one-dimensional unstable center submanifold on $\textbf{S}|_{\Omega_m=0}$, i.e., one solution, called an attractor solution, originates from each fixed point $\text{dS}_\pm$ into **S** on the pure scalar field boundary subset $\Omega_m = 0$. The fixed point $\text{FL}_0$ is a saddle that gives rise to a 1-parameter set of solutions entering **S** (the associated unstable tangent space is

---

[5]A fixed point, sometimes called an equilibrium, critical, or stationary point, is a point $x_0$ in the state space of a dynamical system $\dot{x} = f(x)$ for which $f(x_0) = 0$.

[6]Note that the present de Sitter fixed points are distinct from de Sitter states that are associated with potentials that admit situations for which $dV/d\phi = 0$ for some constant finite value of $\phi$ for which both $V$ and $H$ have constant, bounded, and positive values. In contrast the present de Sitter states correspond to the limits $\dot{\phi} = 0$, $(\phi, V, H) \to (\pm\infty, \infty, \infty)$, and therefore reside on the unphysical boundary $T = 0$.

given by $\Sigma_\dagger = 0$), one being the perfect fluid solution given by $\Omega_\phi = 0, \Omega_m = 1$. The system (22) admits the following conserved quantity when $\Omega_m = 1 - \Sigma_\dagger^2 - X^{2n} > 0$:

$$\Sigma_\dagger^{\gamma_m} X^{(2-\gamma_m)n} \Omega_m^{-1} = \text{const.}, \tag{23}$$

which determines the solution trajectories on the $T = 0$ subset, see Figure 1.



(a) $V(\phi) = \frac{1}{2}m^2\phi^2$, $\gamma_m = \frac{4}{3}$ \qquad (b) $V(\phi) = \frac{1}{4}(\lambda\phi)^4$, $\gamma_m = 1$
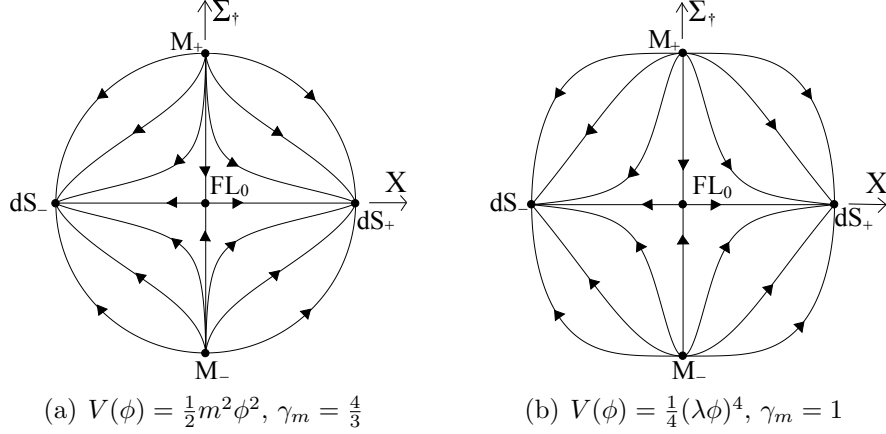
Figure 1: The invariant $T = 0$ boundary subset of $\bar{\mathbf{S}}$ for monomial potentials and a perfect fluid with a linear equation of state. The flows are topologically equivalent for all monomial potentials with $n \geq 1$ and perfect fluids with $0 < \gamma_m < 2$. Depicted are two examples.

The equations on the subset $T = 1$ are given by

$$\frac{d\Sigma_\dagger}{d\bar{\tau}} = -nX^{2n-1}, \tag{24a}$$

$$\frac{dX}{d\bar{\tau}} = \Sigma_\dagger. \tag{24b}$$

This system has a non-hyperbolic fixed point,[7]

$$\text{FL}_1: \quad X = 0, \quad \Sigma_\dagger = 0, \tag{25}$$

with three zero eigenvalues. Fortunately $\text{FL}_1$ resides at the intersection of two invariant subsets: the invariant subset $T = 1$ and the invariant perfect fluid subset $\Omega_\phi = 0, \Omega_m = 1$, and thus, since $T$ is monotone in $\mathbf{S}$, $\text{FL}_1$ attracts at least this orbit. *On $T = 1$ $\text{FL}_1$ is conveniently analyzed by considering eq. (11) on $T = 1$, which yields that*

$$\Omega_\phi = \Sigma_\dagger^2 + X^{2n} = \text{const}, \tag{26}$$

which is an integral of (24), i.e., the subset $T = 1$ is foliated with periodic orbits surrounding the fixed point $\text{FL}_1$, see Figure 2.

---

[7]A fixed point is hyperbolic if the linearization of the dynamical system at the fixed point is a matrix that possesses eigenvalues with non-vanishing real parts; if the linearization leads to one or more eigenvalues with vanishing real parts it is said to be non-hyperbolic.

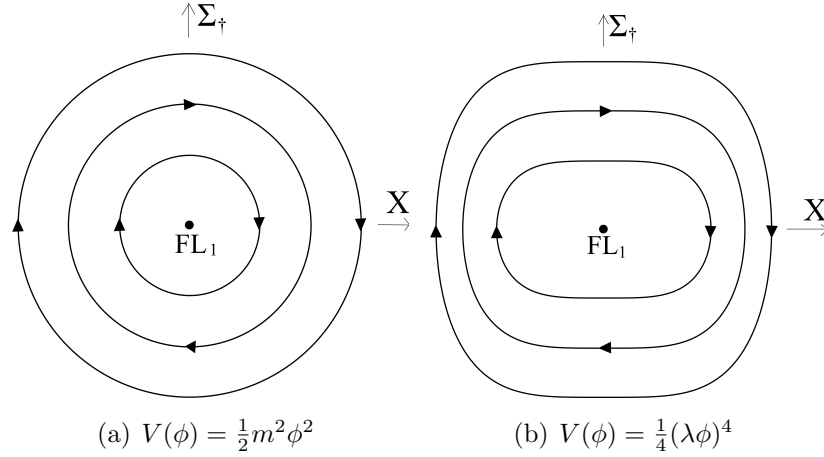(a) $V(\phi) = \frac{1}{2}m^2\phi^2$          (b) $V(\phi) = \frac{1}{4}(\lambda\phi)^4$

Figure 2: The invariant $T = 1$ boundary subset of $\bar{\mathbf{S}}$ for two examples: The potentials $V(\phi) = \frac{1}{2}m^2\phi^2$ and $V(\phi) = \frac{1}{4}(\lambda\phi)^4$ and a perfect fluid (with arbitrary equation of state $0 < \gamma_m < 2$).

To make further progress as regards the global properties of the solution space we need to consider the asymptotic dynamics at early and late times.

## 3.1   Asymptotic dynamics at early times

The linearization of the system (7) at the fixed points $FL_0$ and $M_\pm$ is conveniently described as follows:

$$\frac{1}{T}\frac{dT}{d\bar{\tau}}\bigg|_{FL_0} = \frac{3}{2n}\gamma_m, \qquad\qquad \frac{1}{T}\frac{dT}{d\bar{\tau}}\bigg|_{M_\pm} = \frac{3}{n}, \qquad (27a)$$

$$\frac{1}{\Sigma_\dagger}\frac{d\Sigma_\dagger}{d\bar{\tau}}\bigg|_{FL_0} = -\frac{3}{2}\left(2 - \gamma_m\right), \qquad \frac{1}{1\pm\Sigma_\dagger}\frac{d(1\pm\Sigma_\dagger)}{d\bar{\tau}}\bigg|_{M_\mp} = 3(2 - \gamma_m), \qquad (27b)$$

$$\frac{1}{X}\frac{dX}{d\bar{\tau}}\bigg|_{FL_0} = \frac{3}{2n}\gamma_m, \qquad\qquad \frac{1}{X}\frac{dX}{d\bar{\tau}}\bigg|_{M_\pm} = \frac{3}{n}, \qquad (27c)$$

where the right hand sides constitute the eigenvalues of the fixed points. Hence $FL_0$ is a hyperbolic saddle, with an unstable manifold tangential to $\Sigma_\dagger = 0$, i.e., there is a 1-parameter set of solutions that originate from $FL_0$ entering the state space $\mathbf{S}$ tangentially to $\Sigma_\dagger = 0$. The fixed points $M_\pm$ are hyperbolic sources; it follows from the invariant submanifold structures that there exists a 2-parameter set of solutions entering the interior of the cylinder with $\Omega_m > 0$ from each fixed point $M_\pm$, while a 1-parameter set of solutions originate from each fixed point $M_\pm$ into the boundary subset $\mathbf{S}|_{\Omega_m=0}$.[8]

---

[8]The above results follow from the Hartman-Grobman theorem, which states that in a neighborhood of a hyperbolic fixed point the full nonlinear dynamical system and the linearized system are topologically equivalent, see e.g. [16, 12].

*On* the subset $T = 0$ linearization of the system (22) gives

$$\frac{1}{\Sigma_\dagger} \frac{d\Sigma_\dagger}{d\bar{\tau}}\bigg|_{\mathrm{dS}_\pm} = -3, \tag{28a}$$

$$\frac{1}{1 \mp X} \frac{d(1 \mp X)}{d\bar{\tau}}\bigg|_{\mathrm{dS}_\pm} = -3\gamma_m, \tag{28b}$$

and hence $\mathrm{dS}_\pm$ are hyperbolic sinks on $T = 0$, as illustrated in Figure 1. In the full state space, however, each equivalent fixed point $\mathrm{dS}_\pm$ have an additional zero eigenvalue associated with a one-dimensional so-called center manifold. Fortunately, the center direction lies on the $\mathbf{S}|_{\Omega_m=0}$ subset, and hence we can investigate the center manifold by means of the unconstrained system (14), which will be done in Section 4. There we show that the center manifold of each (equivalent) fixed point $\mathrm{dS}_\pm$ corresponds to a single solution that enters the state space $\mathbf{S}|_{\Omega_m=0}$ (we will even obtain approximate expressions for this solution), and this solution, which hence resides on $\mathbf{S}|_{\Omega_m=0}$, is what is often referred to as the 'attractor' solution. In the full state space $\bar{\mathbf{S}}$ the fixed points $\mathrm{dS}_\pm$ are thus center-saddles.

From these considerations, in combination with the monotonicity of $T$, it follows that all solutions are *past asymptotically self-similar* in the sense that all physical geometrical scale-invariant observables, such as the deceleration parameter $q$, are asymptotically constant. However, there is a twist to this. The geometry of a flat FLRW pure perfect fluid cosmology with a linear equation of state and the geometry of a pure massless scalar field are geometries that admit a proper spacetime transitive homothety group, and such spacetimes are invariant under scalings of the spacetime coordinates. This is the underlying reason why they can be represented by fixed points, but not all fixed points are associated with geometries admitting proper spacetime transitive homothety groups, as exemplified by the de Sitter spacetime. For these spacetimes homothetic scale-invariance is broken by the dimensional cosmological constant, but the 1-parameter set of de Sitter spacetimes (parameterized by $\Lambda$) admits a scaling (self-similar) property that scales $\Lambda$ (i.e., a scaling that maps one de Sitter spacetime to another with a different $\Lambda$), and it is due to this scaling property de Sitter spacetimes can appear as fixed points.

In the present case the fixed points are not in the interior physical state space, but on the unphysical boundary, but they are nevertheless characterized by e.g. the same value of $q$ as the associated physical spacetime. The fact that they in the present context appear on the unphysical boundary has consequences, which we will come back to in a discussion about the de Sitter fixed points in Section 5. Finally we point out that, apart from a set of measure zero, all solutions originate from a massless scalar field state and hence the present models are *past generically massless scalar field dominated.*

## 3.2  Asymptotic dynamics at late times

The equations on the $T = 1$ subset, i.e. equation (24), are equivalent to that of (1c) when setting $H = 0$, i.e. this problem is *exactly* that of an anharmonic oscillator (when $n > 1$; for $n = 1$ the problem is that of a harmonic oscillator). This can be seen from eq. (24), which yields

$$\frac{d^2 X}{d\bar{\tau}^2} + nX^{2n-1} = 0. \tag{29}$$

We will now apply the approximate ideas in Mukhanov [2] to the present exact problem of an anharmonic oscillator. We therefore first multiply the above equation with $X$ and rewrite it as

$$\frac{d}{d\bar{\tau}}\left(X\frac{dX}{d\bar{\tau}}\right) - \left(\frac{dX}{d\bar{\tau}}\right)^2 + nX^{2n} = 0. \tag{30}$$

Each periodic orbit is characterized by a constant value of $\Omega_\phi$ and has an associated time period $P = P(\Omega_\phi)$. The time average of a function $f$ over a period for a periodic orbit characterized by $\Omega_\phi$ is given by

$$\langle f \rangle_{\Omega_\phi} = \int_{\bar{\tau}_0}^{\bar{\tau}_0 + P(\Omega_\phi)} f d\bar{\tau} / P(\Omega_\phi). \tag{31}$$

Taking the time average of eq. (30) for a periodic orbit gives

$$\left\langle \left(\frac{dX}{d\bar{\tau}}\right)^2 \right\rangle = \langle \Sigma_\dagger^2 \rangle = n\langle X^{2n} \rangle, \tag{32}$$

where we for notational convenience from now on drop the subscript $\Omega_\phi$. Again, note that in contrast to the result in [2], this is an exact relation *on* the subset $T = 1$. Using this result on $T = 1$ for a periodic orbit in the definition of $\gamma_\phi$ yields

$$\langle \gamma_\phi \rangle = \left\langle \frac{2\Sigma_\dagger^2}{\Omega_\phi} \right\rangle = \frac{2\langle \Sigma_\dagger^2 \rangle}{\Omega_\phi} = \frac{2\langle \Sigma_\dagger^2 \rangle}{\langle \Sigma_\dagger^2 + X^{2n} \rangle} = \frac{2\langle \Sigma_\dagger^2 \rangle}{\langle \Sigma_\dagger^2 \rangle + \langle X^{2n} \rangle}, \tag{33}$$

which together with (32) leads to

$$\langle \gamma_\phi \rangle = \frac{2n}{n+1} \tag{34}$$

on the subset $T = 1$, i.e., $\langle \gamma_\phi \rangle_{\Omega_\phi} = \langle \gamma_\phi \rangle$ is independent of $\Omega_\phi$. It therefore follows that on average, in the above sense, e.g. $n = 1$ and $n = 2$ on $T = 1$ correspond to dust and radiation, respectively. Note that the result (34) coincides with the approximate heuristic results using proper time given in [1] and [2]; see also [3] for a quite different precise definition of $\langle \gamma_\phi \rangle$, which still yields (34).

Before continuing it is instructive to consider a model that consists of two perfect fluids with constant equation of state parameters $\gamma_1$ and $\gamma_2$. Then $r_m = \rho_1/\rho_2 \propto a^{3(\gamma_2 - \gamma_1)}$ (this expression follows from that $\rho \propto a^{-3\gamma}$, but it can also be obtained from the equation $dr_m/d\tau = 3(\gamma_2 - \gamma_1)r_m$). Since it is not difficult to show that $a \to \infty$ toward the future it follows that $r_m \to \infty$ if $\gamma_2 > \gamma_1$; $r_m \to 0$ if $\gamma_2 < \gamma_1$; $r_m \to$ const. if $\gamma_2 = \gamma_1$, i.e., the fluid with the softest equation of state dominates toward the future.

*Assuming* that asymptotically $\gamma_\phi$ can be replaced with the asymptotic averaged result $\langle \gamma_\phi \rangle = \frac{2n}{n+1}$ in eq. (18b) results in

$$\frac{dr}{d\tau} = 3\left(\gamma_m - \langle\gamma_\phi\rangle\right) r = 3\left(\gamma_m - \frac{2n}{n+1}\right) r, \tag{35}$$

which suggests Theorem 1.1, given in the Introduction, but this is of course no proof. Next we introduce averaging techniques that are subsequently used to provide the proof of this theorem.

**Averaging**

Standard averaging techniques and theorems can be found in Chapter 4 in [33] (the periodic case) and in [32] (the general case). In standard averaging theory, a perturbation parameter $\varepsilon$ plays the key role: roughly speaking, a differential equation of the form $\dot{x} = \varepsilon f(x, t, \varepsilon)$ for $\varepsilon > 0$ is approximated by the averaged equation at $\varepsilon = 0$, i.e., $\dot{y} = \varepsilon\langle f(\bar{y}, ., 0)\rangle$, where the average $\langle.\rangle$ is defined in eq. (31). Furthermore, the error $|x - \bar{y}|$ has to be controlled. In the problem at hand, we consider the differential equations in the variables $\Omega_\phi$ and $T$, where the role of the parameter $\varepsilon$ is played by $1 - T$. Therefore, after setting

$$\varepsilon = 1 - T, \tag{36}$$

we have to prove an averaging theorem for the case where $\varepsilon$ is not a parameter, but a variable that slowly goes to zero. The evolution equation of $\Omega_\phi$ is given in eq. (18), which in terms of $\varepsilon$ takes the form

$$\frac{d\Omega_\phi}{d\bar{\tau}} = 3\varepsilon(\gamma_m - \gamma_\phi)\Omega_\phi(1 - \Omega_\phi), \tag{37}$$

where $\gamma_\phi = 2\Sigma_\dagger^2/\Omega_\phi$. This formulation is problematic due to that $\gamma_\phi$ is not well-defined when $\Omega_\phi$ is zero. We therefore use the following formulation:

$$\frac{d\Omega_\phi}{d\bar{\tau}} = 3\varepsilon(\gamma_m\Omega_\phi - 2\Sigma_\dagger^2)(1 - \Omega_\phi), \tag{38a}$$

$$\frac{d\varepsilon}{d\bar{\tau}} = -\frac{1}{n}\varepsilon^2(1 - \varepsilon)(1 + q), \tag{38b}$$

where $(X, \Sigma_\dagger)$ solves the system (7), $\Omega_\phi = \Sigma_\dagger^2 + X^{2n}$, and

$$q + 1 = \frac{3}{2}\left(2\Sigma_\dagger^2 + \gamma_m(1 - \Omega_\phi)\right). \tag{39}$$

The general idea of averaging is to express $\Omega_\phi$ as

$$\Omega_\phi = y + \varepsilon w(y, \varepsilon, \bar{\tau}), \tag{40}$$

and prove that the evolution of the variable $y$ is approximated at first order by the solution $\bar{y}$ of the averaged equation. For that, consider the average as defined in eq. (31) of the right hand side of eq. (38a). More precisely, considering an equation of the form $y' = \varepsilon f(y, \varepsilon, \bar{\tau}) + \mathcal{O}(\varepsilon^2)$ with $\bar{\tau}$-periodic $f(y, 0, \bar{\tau})$ of period $P = P(y)$, the averaged equation is given by $\bar{y}' = \langle f \rangle(y)$, where $\langle f \rangle(y) := \frac{1}{P}\int_0^P f(y, 0, \bar{\tau})d\bar{\tau}$. According to (34), we have $2\langle \Sigma_\dagger^2 \rangle = \langle \gamma_\phi \rangle \Omega_\phi$, where $\langle \gamma_\phi \rangle = \frac{2n}{n+1}$ is a constant that does not depend on $\Omega_\phi$. Hence the averaged equation reads

$$\frac{d\bar{y}}{d\bar{\tau}} = 3\varepsilon(\gamma_m - \langle \gamma_\phi \rangle)\bar{y}(1 - \bar{y}), \tag{41}$$

while $w$ in eq. (40) will be chosen appropriately in the proof.

**Proof of Theorem 1.1**

To prove Theorem 1.1 we first re-express the theorem in terms of $\Omega_\phi$:

(i) If $\gamma_m - \frac{2n}{n+1} > 0$, initial conditions with positive $\Omega_\phi \leq 1$ and $\varepsilon$ converge for $\bar{\tau} \to \infty$ to the outer periodic orbit with $\Omega_\phi = 1$ tangentially to the slice $\{\varepsilon = 0\}$.

(ii) If $\gamma_m - \frac{2n}{n+1} < 0$, initial conditions with positive $1 - \Omega_\phi$ and $\varepsilon$ converge for $\bar{\tau} \to \infty$ to the center with $\Omega_\phi = 0$ tangentially to the slice $\{\varepsilon = 0\}$.

(iii) If $\gamma_m - \frac{2n}{n+1} = 0$, each periodic orbit on the slice $\{\varepsilon = 0\}$ attracts a 1-parameter set of trajectories with positive initial $\varepsilon$.

*Proof.* Let us first derive a differential equation for $y$ by taking the time derivative of eq. (40):

$$\begin{aligned}
\frac{d\Omega_\phi}{d\bar{\tau}} &= \frac{dy}{d\bar{\tau}} + \frac{d\varepsilon}{d\bar{\tau}}w + \varepsilon\left(\frac{\partial w}{\partial y}\frac{dy}{d\bar{\tau}} + \frac{\partial w}{\partial \bar{\tau}} + \frac{\partial w}{\partial \varepsilon}\frac{d\varepsilon}{d\bar{\tau}}\right) \\
&= \left(1 + \varepsilon\frac{\partial w}{\partial y}\right)\frac{dy}{d\bar{\tau}} + \varepsilon\frac{\partial w}{\partial \bar{\tau}} + \frac{d\varepsilon}{d\bar{\tau}}w + \varepsilon\frac{\partial w}{\partial \varepsilon}\frac{d\varepsilon}{d\bar{\tau}}.
\end{aligned} \tag{42}$$

On the other hand,

$$\begin{aligned}
\frac{d\Omega_\phi}{d\bar{\tau}} &= 3\varepsilon\left(\gamma_m - \langle \gamma_\phi \rangle + \langle \gamma_\phi \rangle - \gamma_\phi\right)(y + \varepsilon w)(1 - y - \varepsilon w) \\
&= 3\varepsilon(\gamma_m - \langle \gamma_\phi \rangle)y(1 - y) + 3(\langle \gamma_\phi \rangle y - 2\Sigma_\dagger^2)(1 - y) \\
&\quad + 3\varepsilon^2(\gamma_m - \gamma_\phi)w(1 - 2y) - 3\varepsilon^3(\gamma_m - \gamma_\phi)w^2.
\end{aligned} \tag{43}$$

Let us now set

$$\frac{\partial w}{\partial \bar{\tau}} = 3(\langle \gamma_\phi \rangle y - 2\Sigma_\dagger^2)(1 - y). \tag{44}$$

Note that for large times $2\Sigma_\dagger^2$ is well approximated by periodic functions with an average $\langle \gamma_\phi \rangle y$. The right hand side of (44) is for large times almost periodic and has an average that is zero so that the variable $w$ is bounded.

As a consequence, the differential equation for the variable $y$ takes the form

$$\frac{dy}{d\bar{\tau}} = \left(1 + \varepsilon \frac{\partial w}{\partial y}\right)^{-1}$$

$$\left\{ 3\varepsilon(\gamma_m - \langle \gamma_\phi \rangle)y(1 - y) \right.$$

$$+ \varepsilon^2 w \left( 3(\gamma_m - \gamma_\phi)(1 - 2y) + \frac{1}{n}(1 - \varepsilon)(1 + q) \right)$$

$$\left. - \varepsilon \frac{\partial w}{\partial \varepsilon}\frac{d\varepsilon}{d\bar{\tau}} - 3\varepsilon^3(\gamma_m - \gamma_\phi)w^2 \right\}. \tag{45}$$

Using the fact that $\varepsilon \frac{\partial w}{\partial \varepsilon}\frac{d\varepsilon}{d\bar{\tau}} = \mathcal{O}(\varepsilon^3)$ and that $\left(1 + \varepsilon \frac{\partial w}{\partial y}\right)^{-1} = 1 - \varepsilon \frac{\partial w}{\partial y} + \mathcal{O}(\varepsilon^2)$ results in the following:

$$\frac{dy}{d\bar{\tau}} = 3\varepsilon(\gamma_m - \langle \gamma_\phi \rangle)y(1 - y)$$

$$+ \varepsilon^2 \left\{ 3w(\gamma_m - \gamma_\phi)(1 - 2y) + \frac{1}{n}(1 - \varepsilon)(1 + q) - 3\frac{\partial w}{\partial y}(\gamma_m - \langle \gamma_\phi \rangle)y(1 - y) \right\}$$

$$+ \mathcal{O}(\varepsilon^3). \tag{46}$$

Next we have to prove that the solution $y$ of this equation and the solution $\bar{y}$ of the averaged equation (41) have the same asymptotics when $\bar{\tau} \to +\infty$. Since the averaged equation (41) is expected to govern the dynamics, we first study the late time behavior of the system

$$\frac{d\bar{y}}{d\bar{\tau}} = 3\varepsilon(\gamma_m - \langle \gamma_\phi \rangle)\bar{y}(1 - \bar{y}), \tag{47a}$$

$$\frac{d\varepsilon}{d\bar{\tau}} = -\frac{1}{n}\varepsilon^2(1 - \varepsilon)(1 + q). \tag{47b}$$

After Euler multiplication by $1/\varepsilon$ (or equivalently, a singular change of time variable $\varepsilon d/d\tau = d/d\bar{\tau}$), this system reads

$$\frac{d\bar{y}}{d\tau} = 3(\gamma_m - \langle \gamma_\phi \rangle)\bar{y}(1 - \bar{y}), \tag{48a}$$

$$\frac{d\varepsilon}{d\tau} = -\frac{1}{n}\varepsilon(1 - \varepsilon)(1 + q). \tag{48b}$$

In cases (i) and (ii), for which $\gamma_m - \langle\gamma_\phi\rangle \neq 0$, the two fixed points of this system are located at $(\varepsilon = 0, \bar{y} = 0)$ and $(\varepsilon = 0, \bar{y} = 1)$. The line $\varepsilon = 0$ is a heteroclinic orbit between these two fixed points, whose direction depends on the sign of $\gamma_m - \langle\gamma_\phi\rangle$.

Undoing the Euler multiplication does not affect the trajectories with positive $\varepsilon$. On the other hand, in the original averaged system (47), the line $\{\varepsilon = 0\}$ is a line of fixed points. Solutions with positive initial $\varepsilon$ will approach the line of fixed points at $\varepsilon = 0$, but slowly slide along this line as $\bar{\tau} \to \infty$ in the direction prescribed by the sign of $\gamma_m - \langle\gamma_\phi\rangle$, and go to the left or right fixed point accordingly.

Next we prove that the variables $y$ and $\Omega_\phi$ follow this evolution. First note that the sequences $\{\varepsilon_n\}_{n\in\mathbb{N}}$, $\{\bar{\tau}_n\}_{n\in\mathbb{N}}$, defined as follows,

$$\begin{cases} \bar{\tau}_0 = 0, \\ \varepsilon_0 > 0, \end{cases} \qquad \begin{cases} \bar{\tau}_{n+1} = \bar{\tau}_n + 1/\varepsilon_n, \\ \varepsilon_{n+1} = \varepsilon(\bar{\tau}_{n+1}), \end{cases} \tag{49}$$

have limits

$$\begin{cases} \lim_{n\to\infty} \bar{\tau}_n = +\infty, \\ \lim_{n\to\infty} \varepsilon_n = 0, \end{cases} \tag{50}$$

since $\varepsilon(\bar{\tau})$ goes to zero when $\bar{\tau}$ goes to infinity. For a sufficiently small $\varepsilon > 0$, eq. (46) guaranties that $y$ is monotone (in- or decreasing, depending on the sign of the quantity $\gamma_m - \langle\gamma_\phi\rangle$) and bounded. Hence $y(\bar{\tau})$ must have a limit when $\bar{\tau} \to \infty$. Next we estimate $\zeta(\bar{\tau}) := y(\bar{\tau}) - \bar{y}(\bar{\tau})$, where $y$ and $\bar{y}$ are trajectories with identical 'initial' conditions at time $\tau_n$:

$$|\zeta(\bar{\tau})| = \Big| \int_{\bar{\tau}_n}^{\bar{\tau}} 3\varepsilon(\gamma_m - <\gamma_\phi>)(y - \bar{y})\underbrace{(1 - (y + \bar{y}))}_{|.|\leq 1}\, ds$$

$$+ \int_{\bar{\tau}_n}^{\bar{\tau}} (\varepsilon^2 \underbrace{h(y, w, \varepsilon, s)}_{|.|\leq M} + \mathcal{O}(\varepsilon^3))\, ds \Big| \tag{51}$$

$$\leq 3C\varepsilon_n \int_{\bar{\tau}_n}^{\bar{\tau}} |\zeta(s)|\, ds + \varepsilon_n^2 \int_{\bar{\tau}_n}^{\bar{\tau}} M\, ds + \mathcal{O}(\varepsilon_n^3))$$

$$\leq 3C\varepsilon_n \int_{\bar{\tau}_n}^{\bar{\tau}} |\zeta(s)|\, ds + \varepsilon_n^2 M(\bar{\tau} - \bar{\tau}_n) + \mathcal{O}(\varepsilon_n^3),$$

for $\bar{\tau} \geq \bar{\tau}_{n+1}$, where we used the fact that $|(\gamma_m - <\gamma_\phi>)| \leq C$ with $C > 0$ constant. Applying Gronwall's Lemma (see Lemma 4.1.2 in [33], or p. 37 in [34]), results in

$$|\zeta(\bar{\tau})| \leq \frac{M}{3}\varepsilon_n(\exp(3C\varepsilon_n(\bar{\tau} - \bar{\tau}_n)) - 1) + \mathcal{O}(\varepsilon^2). \tag{52}$$

Hence for $\bar{\tau} - \bar{\tau}_n \in [0, 1/\varepsilon_n]$, i.e. $\bar{\tau} \in [\bar{\tau}_n, \bar{\tau}_{n+1}]$, the inequality $|\zeta(\bar{\tau})| \leq K\varepsilon_n$ holds for a positive constant $K$. Letting $n$ go to infinity implies that $\zeta$ tends to zero when $\bar{\tau}$ goes to infinity. Therefore $y$ and $\bar{y}$ have the same limit as $\bar{\tau} \to \infty$, i.e. 0 or 1 depending on the sign of the quantity $\gamma_m - \langle\gamma_\phi\rangle$. Finally, recall that $\Omega_\phi = y + \varepsilon w$; from the

triangle inequality, and $\varepsilon \to 0$ when $\bar{\tau} \to \infty$, it follows that $\Omega_\phi$ also converges to 0 or 1 according to the sign of $\gamma_m - \langle \gamma_\phi \rangle$. This completes the proof of the theorem for the non-critical cases (i) and (ii) for which $\gamma_m - \langle \gamma_\phi \rangle \neq 0$.

Let us now consider the critical case (iii), for which $\gamma_m = \langle \gamma_\phi \rangle = 2n/(n+1)$. In this case the right hand side of the averaged equation (41) vanishes. Furthermore, the evolution equation (46) for $y$ becomes

$$\frac{dy}{d\bar{\tau}} = \varepsilon^2 \left\{ 3w(\gamma_m - \gamma_\phi)(1 - 2y) + \frac{1}{n}(1 - \varepsilon)(1 + q) \right\} + \mathcal{O}(\varepsilon^3) \tag{53}$$

Let us first consider the average of the right hand side. We therefore define

$$g(y, w, \varepsilon, \bar{\tau}) = 3w(\gamma_m - \gamma_\phi)(1 - 2y) + \frac{1}{n}(1 - \varepsilon)(1 + q), \tag{54}$$

and compute its average at $\varepsilon = 0$, where $\Sigma_\dagger^2$ is a periodic function and $\langle 2\Sigma_\dagger^2 \rangle = \langle \gamma_\phi \rangle y$,

$$
\begin{aligned}
\langle g \rangle (y, w) &= \frac{1}{P} \int_0^P g(y, w, 0, \bar{\tau}) d\bar{\tau} \\
&= 3w \underbrace{(\gamma_m - \langle \gamma_\phi \rangle)}_{=0}(1 - 2y) + \frac{1}{n}\langle 1 + q \rangle \\
&= \frac{3}{2n} \frac{1}{P} \int_0^P (2\Sigma_\dagger^2 + \gamma_m(1 - y)) d\bar{\tau} \\
&= \frac{3}{2n} \left( \underbrace{(\gamma_m - \langle \gamma_\phi \rangle)}_{=0} y + \gamma_m \right) \\
&= \frac{3}{2n}\gamma_m
\end{aligned}
\tag{55}
$$

Note that in the critical case, $\frac{3}{2n}\gamma_m = \frac{3}{2n}\langle \gamma_\phi \rangle = \frac{3}{2n}\frac{2n}{(n+1)} = \frac{3}{n+1}$. We therefore obtain the following averaged system, expected to give the leading order approximation:

$$\frac{d\bar{z}}{d\bar{\tau}} = \varepsilon^2 \frac{3}{n+1}, \tag{56a}$$

$$\frac{d\varepsilon}{d\bar{\tau}} = -\frac{3}{n(n+1)}\varepsilon^2(1 - \varepsilon). \tag{56b}$$

Again we study the dynamics on a Euler multiplied version of this system, i.e. in the time variable $\varepsilon d/d\tau = d/d\bar{\tau}$:

$$\frac{d\bar{z}}{d\tau} = \varepsilon \frac{3}{n+1}, \tag{57a}$$

$$\frac{d\varepsilon}{d\tau} = -\frac{3}{n(n+1)}\varepsilon(1 - \varepsilon). \tag{57b}$$

The linearization at the line of fixed points $\{\varepsilon = 0\}$ is

$$
\begin{pmatrix}
0 & \frac{3}{(n+1)} \\
0 & -\frac{3}{n(n+1)}
\end{pmatrix}
$$

This linearization admits one eigenvalue that is zero with a corresponding eigenvector that is parallel to the line of fixed points, and a stable (i.e. negative) eigenvalue $\lambda = -\frac{3}{n(n+1)}$, with a corresponding eigenvector $(z = -n, \varepsilon = 1)$ pointing toward the inside of the cylinder (i.e. the line of fixed points of the system (57) is transversally hyperbolic). Hence each fixed point $(\bar{z}_0, 0)$ has a one-dimensional stable manifold, i.e., there exists a trajectory $\bar{z}(\tau)$ that solves the averaged system (57) with a positive initial $\varepsilon$ and converges to $(\bar{z}_0, 0)$ for each $\bar{z}_0$ as $\tau \to \infty$. This asymptotic behavior is not affected by transforming the equations back to the time variable $\bar{\tau}$.

A straightforward estimation of the term $\mathcal{O}(\varepsilon^3)$ provides bootstrapping sequences $\{\bar{\tau}_n\}_{n \in \mathbb{N}}$ and $\{\varepsilon_n\}_{n \in \mathbb{N}}$, defined similarly as in the non-critical case (49). In other words, we obtain a pseudo-trajectory $\{\Omega_\phi^n(\bar{\tau})\}$ of the original system (38) with

$$
\Omega_\phi^n(\bar{\tau}_n) = \bar{z}(\bar{\tau}_n), \qquad \forall \bar{\tau} \in [\bar{\tau}_n, \bar{\tau}_{n+1}], \qquad |\Omega_\phi^n(\bar{\tau}) - \bar{z}(\bar{\tau})| < K\varepsilon_n, \qquad (58)
$$

for a constant $K$. By regularity of the flow and compactness of the cylinder, there is an initial data whose trajectory $\Omega_\phi(\bar{\tau})$ under the flow of the original equation (38) shadows the above pseudo-trajectory in the following sense:

$$
\forall n \in \mathbb{N}, \qquad \forall \bar{\tau} \in [\bar{\tau}_n, \bar{\tau}_{n+1}], \qquad |\Omega_\phi^n(\bar{\tau}) - \Omega_\phi(\bar{\tau})| < K\varepsilon_n. \qquad (59)
$$

By the triangle inequality, $|\Omega_\phi^n(\bar{\tau}) - \bar{z}(\bar{\tau})| \to 0$ as $\bar{\tau} \to \infty$; therefore, for each $\bar{z}_0 \in [0, 1]$, there exists a trajectory that is limiting to the periodic trajectory at $\varepsilon = 0$, characterized by $\Omega_\phi = \bar{z}_0$. Translating these results into the state space of (7) concludes the proof of case (iii). $\qquad \square$

Expressing these results for orbits with $0 < \Omega_m < 1$ and $0 < T < 1$ in terms of formal global future attractors $\mathcal{A}_+$ of the global dynamical system (7) leads to:[9]

(i) $\mathcal{A}_+ = \bar{\mathbf{S}}|_{T=1, \Omega_m=0}$        if    $\gamma_m > \frac{2n}{n+1}$,

(ii) $\mathcal{A}_+ = \bar{\mathbf{S}}|_{T=1, \Omega_\phi=0} = \mathrm{FL}_1$    if    $\gamma_m < \frac{2n}{n+1}$,

(iii) $\mathcal{A}_+ = \bar{\mathbf{S}}|_{T=1}$           if    $\gamma_m = \frac{2n}{n+1}$.

The above results are illustrated by the numerical examples that are depicted in Figure 3.

---

[9]Loosely speaking, in dynamical systems theory attractor behavior describes situations where a collection of state space points evolve into a certain 'attractor' region from which they never leave. For a formal definition of a dynamical systems attractor, see e.g. [17], and references therein.

(a) The scalar field boundary

(b) $\gamma_m = \frac{3}{2}$

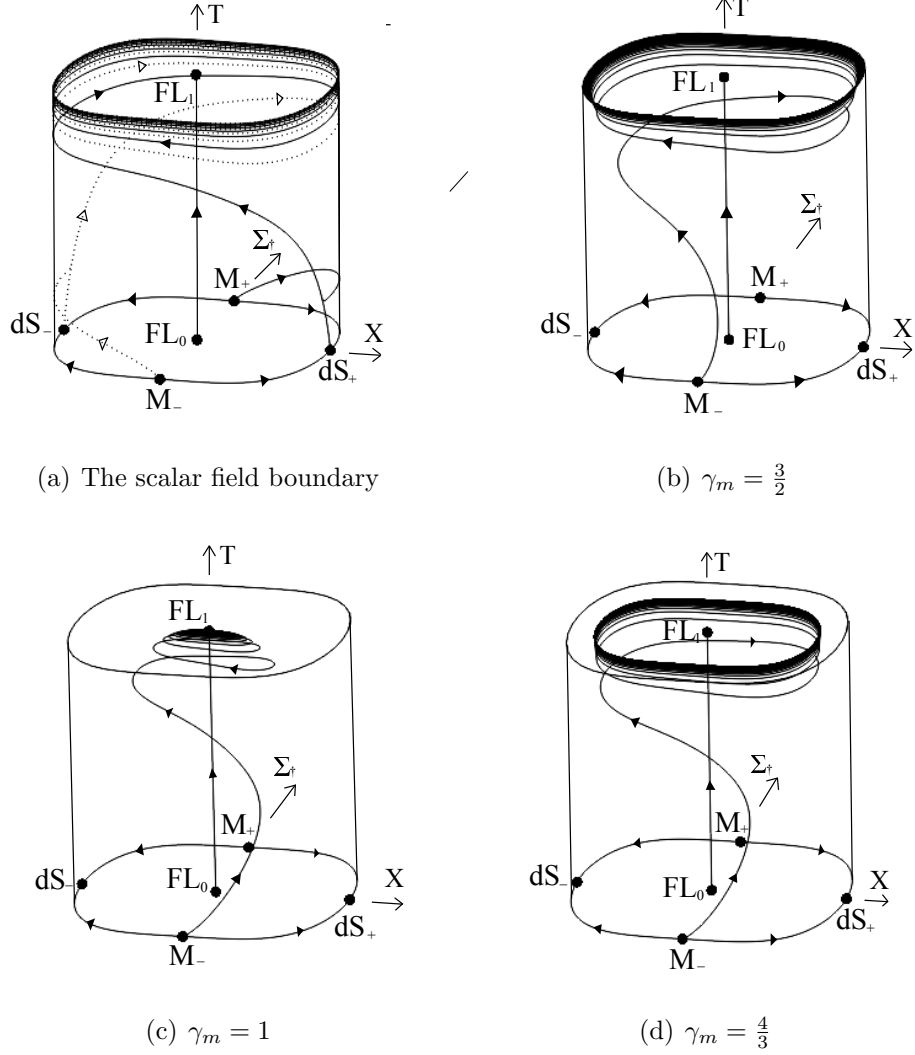(c) $\gamma_m = 1$

(d) $\gamma_m = \frac{4}{3}$

Figure 3: Solutions for the scalar field potential $V(\phi) = \frac{1}{4}(\lambda\phi)^4$ for various matter equation of states. The first picture describes a solution and the attractor solutions on the scalar field boundary. The other figures depict a typical solution that illustrates the behavior at late times for cases (i) (i.e., $\gamma_m > \frac{2n}{n+1}$), (ii) (i.e., $\gamma_m < \frac{2n}{n+1}$), and (iii) (i.e., $\gamma_m = \frac{2n}{n+1}$).

**Physical Interpretation**

The present results have physical consequences. The solutions approach $(H, \phi, \dot{\phi}, \rho_m) = (0, 0, 0, 0)$ toward the future, which is the Minkowski solution of the system (1). The Minkowski solution admits an 11-dimensional homothety group and is therefore an example of a self-similar spacetime. However, the asymptotic future state for solutions in case (i), with $\gamma_m > \frac{2n}{n+1}$ and $\Omega_\phi > 0$, is the periodic orbit at $\Omega_\phi = 1 = T$,

and hence, since the future asymptotic behavior is described by a limit cycle, it follows that the deceleration parameter $q$ oscillates toward the future (this is also obviously true for the orbits on the subset $\Omega_\phi = 1$). The solutions thus approach the Minkowski spacetime in a foliation that is induced by the present models in a manner where the self-similar nature of the Minkowski spacetime is not manifest and thus we say that these models exhibit *future asymptotic manifest self-similarity breaking.*[10]

Physically, case (ii), for which $\gamma_m < \frac{2n}{n+1}$, has the simplest asymptotic regime. The future state for this case when $\Omega_m > 0$ is the fixed point $\mathrm{FL}_1$ for which $q = \frac{1}{2}(3\gamma_m - 2)$. This state describes the flat perfect fluid model with equation of state parameter $\gamma_m$. Since this model is self-similar, the solutions asymptotically approach the Minkowski spacetime in a manifest self-similar manner and we therefore say that the present class of models are *future asymptotically* (manifestly) *self-similar.*

Case (iii), where $\gamma_m = \frac{2n}{n+1}$, implies that (with the exception of the perfect fluid solution with $\Omega_\phi = 0$) all solutions oscillate asymptotically toward the future and thus this case is also characterized by future asymptotic manifest self-similarity breaking. Since asymptotic manifest self-similarity, and breaking thereof, plays an important role in physics as a whole, it is of considerable interest to note the above features.

Furthermore, recall that the case $\gamma_m = \frac{2}{3}$ is equivalent to a pure scalar field case in an open FLRW model. As a consequence *all* monomial potentials (with $n \geq 1$) for these models lead to that the future end state is given by the fixed point $\mathrm{FL}_1$, which in this context is associated with a Milne state.

We are now finally in a position to describe the global solution space and its features. There is a 1-parameter set of solutions that originate from the fixed point $\mathrm{FL}_0$, corresponding to an initial perfect fluid dominated state, into the state space **S**; two equivalent 2-parameter sets of solutions that originate from each of the equivalent fixed points $\mathrm{M}_\pm$, corresponding to a self-similar initial massless scalar field dominated state, where two equivalent 1-parameter subsets, belonging to each of these sets of solution, reside on the scalar field boundary $\Omega_\phi = 1$; finally, there are two equivalent attractor solutions residing on $\Omega_\phi = 1$ that originate from each of the fixed points $\mathrm{dS}_\pm$, thus exhibiting an initial de Sitter state in the sense previously discussed. The future state of all orbits in **S** resides on the subset $T = 1$, where the precise asymptotic location on $T = 1$ depends on the relation between the monomial potential exponent $2n$ and the equation of state parameter $\gamma_m$ according to

---

[10]Asymptotic (continuous) manifest self-similarity here implies that physical geometrical scale-invariant observables such as the deceleration parameter $q$ take asymptotic constant values, but since the future attractor is a limit cycle it follows that $q$ is asymptotically oscillating, i.e., asymptotic manifest self-similarity is broken. For another example of future asymptotic self-similarity breaking in cosmology, see [19]. Note that asymptotic manifest self-similarity is a complicated issue in the present asymptotic Minkowski case due that the only metrics with no conformal scalars (and hence the only admitting a local conformal group not conformally isometric) are either conformal to the plane wave metric with parallel rays or conformally Minkowski, see [20, 21].

Theorem 1.1.

In all three cases (i), (ii), and (iii) there exists an open set of solutions that is close to the attractor solutions at some intermediate stage of their evolution, but there also exists an open set of solutions that is not close to the attractor solutions. Furthermore, although there exists an open set of solutions that is close to the attractor solutions at late times in case (i) this is not true for case (ii) where each (equivalent) attractor solution only acts as a kind of 'saddle.' In addition, note that the variables $T, \Sigma_\dagger, X$ can be locally expressed in terms of the physical quantities $H, q, \Omega_m$. By imposing a Euclidian measure on the space described by $H, q, \Omega_m$ one finds that 'most' of the evolution of 'most' solutions is not governed by the 'attractor' solution; the addition of a degree of freedom, in this case associated with a perfect fluid, has aggravated the situation for arguments that attempt to establish that attractor solutions in some sense are attractors.[11] Nevertheless, attractor solutions are likely to continue to generate considerable attention, and thus there is a need to describe them accurately, which is the topic of the next section.

# 4   Attractor solution approximants

In this section we will introduce and compare several analytical approximation schemes that describe the attractor solution. Since the two equivalent attractor solutions are just the center manifolds of $dS_\pm$, we begin with a direct approach of approximately obtaining these center manifolds by means of center manifold theory. For presentations of center manifold analysis, see e.g., [26, 16], and for applications in cosmology, e.g., [18, 28, 12].

## 4.1   Center manifold approximants

The equivalent center manifolds of $dS_\pm$ reside on the scalar field subset $\Omega_m = 0$ and therefore it suffices to study the equations on this subset. In [12] it was shown that for quadratic potentials the center manifold expansion using the bounded system (14) for $n = 1$ resulted in a larger range than the expansion based on the unbounded system (19). However, it was also shown that by using these expansions to produce so-called Padé approximants resulted in much better approximations, both as regards accuracy and range. Moreover, the Padé approximants for the system (19) gave the same expressions as the Padé approximants obtained from (14) (or, more accurately, they produced the converging subset of Padé approximants associated with (14)), but in a simpler form. Thus the most useful results from center manifold analysis are obtained by performing such an analysis for the un-

---

[11]For further discussions about the meaning of 'attractor solutions' and measures, see [12] and the recent papers by Remmen and Carroll [22, 23] and by Corichi and Sloan [24], and references therein.

bounded system (19), followed by an introduction of Padé approximants, instead of using (14).

Due to the discrete symmetry, we can, without loss of generality, restrict the center manifold analysis to the fixed point $dS_+$ at $\theta = 0 = \tilde{T}$. A linearization of the system (19) at this fixed point yields

$$E^s = \{(\tilde{T}, \theta)|\tilde{T} = 0\}, \tag{60a}$$

$$E^c = \{(\tilde{T}, \theta)|\sqrt{n}\tilde{T} + 3\theta = 0\}, \tag{60b}$$

where $E^s$ and $E^c$ denote the tangential stable and center subspaces, respectively. Since the tangential center subspace is given by $\sqrt{n}\tilde{T} + 3\theta = 0$, we introduce

$$v = \tilde{T} + \frac{3}{\sqrt{n}}\theta \tag{61}$$

as a new variable that replaces $\theta$ in order to study the center manifold $W^c$, with the tangent space $E^c$ at $(\tilde{T}, v) = (0, 0)$. As follows from (19), this leads to the transformed system

$$\frac{d\tilde{T}}{d\tau} = \frac{3}{n}\tilde{T}\left(1 - \cos^{2n}\theta\right), \tag{62a}$$

$$\frac{dv}{d\tau} = \frac{3}{\sqrt{n}}\left(\frac{1}{\sqrt{n}}\tilde{T}\left(1 - \cos^{2n}\theta\right) - \tilde{T}F(\theta) - \frac{3}{2n}F^2(\theta)\sin 2\theta\right), \tag{62b}$$

where $\theta = \frac{\sqrt{n}}{3}(v - \tilde{T})$. The linearization of eq. (62b) yields $\frac{dv}{d\tau} = -3v$, while eq. (62a) only has higher order terms. The center manifold $W^c$ can be obtained as the graph $v = h(\tilde{T})$ near $(\tilde{T}, v) = (0, 0)$ (i.e., use $\tilde{T}$ as an independent variable), where $h(0) = 0$ (fixed point condition) and $\frac{dh}{d\tilde{T}}(0) = 0$ (tangency condition). Inserting this relationship into eq. (62) and using $\tilde{T}$ as the independent variable leads to

$$\frac{1}{\sqrt{n}}\tilde{T}\left(1 - \cos^{2n}\theta\right)\left(\frac{dh}{d\tilde{T}} - 1\right) + \tilde{T}F(\theta) + \frac{3}{2n}F^2(\theta)\sin 2\theta = 0, \tag{63}$$

where $\theta = \frac{\sqrt{n}}{3}(h(\tilde{T}) - \tilde{T})$.

Solving the above nonlinear ordinary differential equation amounts to finding the attractor solution, which for the present class of problems does not seem likely to be possible. Instead the equation can be solved approximately by representing $h(\tilde{T})$ as a formal truncated power series and by Taylor expanding the expressions involving $\theta$ (and subsequently replace $\theta$ with its power series expression in $\tilde{T}$), which makes it possible to algebraically solve for the coefficients in the formal series. Before doing this, it is useful to note that all coefficients in the above equation are odd in terms of $\tilde{T}$ and $\theta$, and as a consequence the power series for $h$ consists of odd powers of $\tilde{T}$, since it is only then $\frac{dh}{d\tilde{T}}$ results in even powers (odd powers for $\frac{dh}{d\tilde{T}}$, and hence even powers for $h$, are clearly zero due to the above properties). Furthermore, it follows

from the tangency condition that the series for $h$ in odd powers of $\tilde{T}$ begins with a cubic term. Hence

$$h(\tilde{T}) = \sum_{i=1}^{n} a_i \tilde{T}^{2i+1} + \mathcal{O}(\tilde{T}^{2n+3}) = \tilde{T} \sum_{i=1}^{n} a_i x^i + \mathcal{O}(\tilde{T}^{2n+3}) \qquad \text{as} \qquad \tilde{T} \to 0, \quad (64)$$

where the series for $h(T)$ is truncated at some chosen order and where we have introduced $x = \tilde{T}^2$. Inserting this into a Taylor expansion of eq. (63) and algebraically solving for the coefficients leads to

$$\theta \approx -\frac{\sqrt{n}}{3} \tilde{T} f(x),$$
$$f(x) = 1 + \frac{n}{108} \left[ (3n-7)x + \frac{n}{360} (65n^2 - 570n + 1081)x^2 \right], \tag{65}$$

where we have chosen to truncate the series for $\theta$ at 5th order in $\tilde{T}$.

To improve the range and accuracy of the above approximation for the attractor solution we construct the $[1/1]_f(x)$ Padé approximant, which leads to the following approximate expression for $\theta$:[12]

$$\theta \approx -\frac{\sqrt{n}}{3} \tilde{T}[1/1]_f(x), \qquad [1/1]_f(x) = \frac{1 - \frac{n}{36(3n-7)} \left( \frac{7}{2}n^2 - 43n + \frac{2753}{30} \right) x}{1 - \frac{n}{36(3n-7)} \left( \frac{13}{2}n^2 - 57n + \frac{1081}{10} \right) x}. \tag{66}$$

When this is subsequently expressed in $T$, i.e., $\tilde{T} = T/(1-T)$ and $x = T^2/(1-T)^2$, this yields a curve $\theta(T)$ which approximates the attractor solution in the state space **S** on the boundary $\Omega_m = 0$. The case $n = 1$ was dealt with in Figures 5 and 14 in [12], where these approximations curves for the attractor solution, as well as those obtained by considering higher order expansions, were compared with the numerically computed attractor solution. To obtain explicit curves in our state space picture we need to specify $n$. To avoid details, we in this paper only compare the approximate solution curves with the numerically computed attractor solution for some representative values of $n$ for the above $[1/1]_f(x)$ Padé approximant in subsection 4.4 below; although it should be pointed out that higher order Padé approximants give better, although more complicated, results.

Ref. [12] also illustrates that nonlinear transformations might have two important features. First, they affect analytical or numerical computations and therefore a suitable choice of variables can make a problem more tractable. Second, they affect approximations and a suitable choice of variables can lead to better approximations for solutions like the attractor solution. We will therefore next consider an approximation scheme based on the variables $\Sigma_\dagger$ and $X$ instead of $\theta$.

---

[12]A Padé approximant of order $(m, n)$ of a function $f(x)$, denoted by $[m/n]_f(x)$, is associated with a truncated Taylor series $f \approx c_0 + c_1 x + c_2 x^2 + \cdots + c_{m+n} x^{m+n}$ and given by the polynomials $P_m(x) = p_0 + p_1 x + p_2 x^2 + \cdots + p_m x^m$ and $Q_n(x) = q_0 + q_1 x + q_2 x^2 + \cdots + q_n x^n$ according to $[m/n]_f(x) = \frac{P_m(x)}{Q_n(x)}$, such that $Q_n(x)(c_0 + c_1 x + c_2 x^2 + \cdots + c_{m+n} x^{m+n}) = P_m(x)$, where coefficients with the same powers of $x$ are equated up through $m + n$. For details and examples, see [29, 30, 27, 12] and references therein.

## 4.2   Series expansion approximants

As in the previous case we use a system adapted to the dynamics at early times and we therefore use $\tilde{T}$, but $\theta$ is replaced with $\Sigma_\dagger$ and $X$, i.e., we consider the system (17). We are interested in finding new approximations for the attractor solution, and inspired by the result in eq. (65) we assume that $\Sigma_\dagger$ and $X$ can be written as formal truncated series in $\tilde{T}$. These series are subsequently inserted in (17), but since we are interested in the attractor solution, which resides on the $\Omega_m = 0$ boundary, we also require that the constraint $\Sigma_\dagger^2 + X^{2n} = 1$ is satisfied. The analysis is simplified by noting that it follows from the system (17) that $\Sigma_\dagger$ must have only odd terms while $X$ have only even terms in their series expansions in $\tilde{T}$. Moreover, since we choose, without loss of generality, to consider the solution that originates from the $\mathrm{dS}_+$ fixed point it follows that to lowest order $\Sigma_\dagger = 0, X = 1$. Algebraically solving for the coefficients, and writing $\tilde{T}^2 = x$ as before, leads to

$$\Sigma_\dagger \approx -\frac{n}{3}\tilde{T}f(x), \qquad f(x) = 1 - \frac{n}{18}x + \frac{n^2}{648}(17 - 6n)x^2, \tag{67a}$$

$$X \approx 1 - \frac{n}{18}x + \frac{n^2}{648}(5 - 2n)x^2, \tag{67b}$$

where we have chosen to truncate the series for $f(x)$ and $X(x)$ at 2nd order in $x$.

To improve the range and accuracy we calculate the $[1/1]_f(x)$ and $[1/1]_X(x)$ Padé approximants, which yield the following approximate expressions

$$\Sigma_\dagger \approx -\frac{n}{3}\tilde{T}\left[\frac{1 + \frac{n}{12}(5 - 2n)x}{1 + \frac{n}{36}(17 - 6n)x}\right], \tag{68a}$$

$$X \approx \frac{1 + \frac{n}{36}(3 - 2n)x}{1 + \frac{n}{36}(5 - 2n)x}. \tag{68b}$$

Note that for small values of $\tilde{T}$ in the neighborhood of $\mathrm{dS}_+$ we obtain $X = 1 - \frac{n}{18}\tilde{T}^2 = \cos\theta \approx 1 - \frac{1}{2}\theta^2$, which gives $\theta = -\frac{\sqrt{n}}{3}\tilde{T}$, which is just the tangency condition for the center manifold of $\mathrm{dS}_+$. Replacing $\tilde{T}$ and $x$ with $T$ in (68) yield two curves in the state space $\mathbf{S}$ on the scalar field subset $\Omega_m = 0$, one for the approximation of $X$ and one for the approximation of $\Sigma_\dagger$, both approximating the attractor solution.

To obtain accurate numerical results for the attractor solution it is preferable to use the unconstrained system (14) rather than (7) subjected to the constraint $\Sigma_\dagger^2 + X^{2n} = 1$, especially when $\gamma_m < \frac{2n}{n+1}$ since the constraint surface then becomes unstable for sufficiently large $T$. The above results are translated into the corresponding $\theta(T)$ curves via $\theta = -\arccos X$ (the minus sign is due to that $\theta < 0$ and taking the default branch) and implicitly via $F(\theta)\sin\theta = -\frac{n}{3}\left(\frac{T}{1-T}\right)f$, where $X(x(T))$ and $f(x(T))$ are obtained by replacing $x$ with $T$ in (67) and (68), which lead to approximations that subsequently can be compared with the numerically computed attractor solution. Below, in subsection 4.4 we for brevity only discuss the Padé approximant given in eq. (68a) for some representative values of $n$.

As a final remark, note that the lowest order expansion just gives $X = 1$, which is equivalent to $\Sigma_\dagger = 0$, since $X^{2n} = 1 - \Sigma_\dagger^2$ on the scalar field boundary. The condition $\Sigma_\dagger = 0$ and $X = 1$ describes a straight vertical line in $\bar{\mathbf{S}}$, corresponding to $q = -1$, originating from $\mathrm{dS}_+$, which apart from $\mathrm{dS}_+$ is not a good approximation for the attractor solution. This is in contrast with the previous center manifold expansion, which is given by a unique curve $\theta(T)$, which to all orders in the limit of small $T$ is tangent to the center manifold.

Next we turn to approximations based on the slow-roll approximation and its extensions.

## 4.3   Slow-roll based approximants

We here extend the work in [25] and [12] to general $n$ and to higher order by approximating $H^2(\phi)$ with so-called slow-roll Hubble expansions, and illustrate this class of approximations in our global state space picture. To facilitate comparison with the inflationary literature, we initially keep the coupling constant $\kappa = 8\pi G = 8\pi m_{\mathrm{Pl}}^{-2}$ in the slow-roll Hubble expansion formulas below. The approach developed in [25] is based upon a hierarchy of slow-roll parameters, the first being

$$\epsilon_H = 3 \left( \frac{\frac{1}{2}\dot{\phi}^2}{\frac{1}{2}\dot{\phi}^2 + V(\phi)} \right) = 1 + q, \qquad \eta_H = -3 \left( \frac{\ddot{\phi}}{3H\dot{\phi}} \right), \tag{69}$$

which are assumed to be small. These parameters allow one to produce a truncated expansion for the Hubble variable in terms of $\phi$, which for the present monomial scalar field potential is given by (following the prescription given in [25], which we refer to for details):

$$3H^2 \approx \frac{\kappa}{2n}(\lambda\phi)^{2n} f(y) = \kappa V(\phi) f(y),$$

$$f(y) = 1 + y + \left(1 - \frac{2}{n}\right) y^2 + \left(1 - \frac{3}{n}\right)^2 y^3 + \left(\left(1 - \frac{4}{n}\right)^3 + \frac{2}{n^3}\right) y^4 + \mathcal{O}\left(y^5\right)$$

$$\tag{70}$$

where we have found it convenient to define a quantity $y$ according to

$$y = \frac{2n^2}{3\kappa\phi^2}. \tag{71}$$

Note that the 2nd (3rd) order term is zero in (70) when $n = 2$ ($n = 3$). The above series expansion contains no parameters and thus it can only describe a single solution, moreover, for the series expansion to make sense requires that $y$ is small and hence that $\phi$ is large, which leads to that $H$ is large, i.e., for the present models the Hubble slow-roll expansion attempts to approximately describe the dynamics at early times for a certain solution, but which one?

In terms of $T$ and $X$, and therefore in $T$ and $\theta$, the definitions in eq. (4) lead to that the Hubble expansion (70) can be written on the form (from now on we set $\kappa = 1$)

$$1 \approx X^{2n} f(y) = \cos^{2n} \theta f(y) \quad \text{where} \quad y = \left(\frac{n\tilde{T}}{3X}\right)^2 = \left(\frac{n\tilde{T}}{3\cos\theta}\right)^2, \qquad (72)$$

(as usual, $\tilde{T} = T/(1-T)$) where each order yields an implicit relation for a curve on the scalar field boundary, although it can be used to provide a series expansion for $X$ in terms of $\tilde{T}$ for small $\tilde{T}$ and hence for small $T$.

Note that just as in the previous approximation scheme, the zeroth order Hubble expansion just gives $X^{2n} = 1$, which, as stated earlier, is not a good approximation for the attractor solution. Nevertheless, this approximation is what is sometimes referred to as the slow-roll Hubble approximation, see e.g. [31]. At first order, when $f(y) = 1 + y$, eq. (72) results in

$$\frac{1 - X^{2n}}{X^{2(n-1)}} = \frac{1 - \cos^{2n}\theta}{\cos^{2(n-1)}\theta} = \left(\frac{n}{3}\tilde{T}\right)^2. \qquad (73)$$

Without loss of generality, consider the neighborhood of $\mathrm{dS}_+$; then the above expression yields the limit (beyond the $\mathrm{dS}_+$ point itself)

$$\theta \approx -\frac{\sqrt{n}}{3}\tilde{T} \approx -\frac{\sqrt{n}}{3}T, \qquad (74)$$

which is the tangency condition for the center submanifold of $\mathrm{dS}_+$. Thus all curves associated with eq. (70) originate from $\mathrm{dS}_\pm$; furthermore, all curves associated with orders larger than zero are tangential to the attractor solutions in the small $T$-limit toward $\mathrm{dS}_\pm$.

To improve the range and rate of convergence one can compute Padé approximants for the Hubble expansion for $f(y)$, i.e.,

$$3H^2 \approx \frac{1}{2n}(\lambda\phi)^{2n}[L/M]_f(y) = V(\phi)[L/M]_f(y), \qquad (75)$$

where

$$[1/1]_f(y) = \frac{1 + \frac{2}{n}y}{1 - \left(1 - \frac{2}{n}\right)y}, \qquad (76a)$$

$$[2/2]_f(y) = \frac{1 - \frac{5}{2n} - \left(1 - \frac{11}{n} + \frac{22}{n^2}\right)y + \frac{8}{n^2}\left(1 - \frac{43}{16n}\right)y^2}{1 - \frac{5}{2n} - 2\left(1 - \frac{27}{4n} + \frac{11}{n^2}\right)y + \left(1 - \frac{9}{n} + \frac{25}{n^2} - \frac{43}{2n^3}\right)y^2}. \qquad (76b)$$

In Ref. [12], these approximations have been compared with the numerically computed attractor solutions in detail for $n = 1$, see Fig. 7 and Table 3 of [12].[13]

---

[13]In [12] the authors used the slow-roll parameters to introduce so-called Canterbury approximants in order to improve the range and accuracy of the approximations. We find that Canterbury approximants give more cumbersome and poorer approximations than the corresponding Padé approximants when they differ (to lowest order they agree with each other).

Let us now turn to what is referred to as *the slow-roll approximation* in e.g. [31]. This approximation is obtained by inserting the lowest order Hubble expansion approximant $H = \sqrt{V(\phi)/3}$ into

$$\dot{\phi} = -2\frac{\partial H}{\partial \phi}, \tag{77}$$

which yields

$$\dot{\phi} \approx -\sqrt{\frac{2n}{3}}\lambda^n \phi^{n-1} \tag{78}$$

in the present case with a monomial potential. Expressed in terms of the variables $\Sigma_\dagger$ and $X$, this gives

$$\Sigma_\dagger \approx -\frac{n}{3}X^{n-1}\tilde{T}, \tag{79}$$

which when squared leads to

$$\frac{\Sigma_\dagger^2}{X^{2(n-1)}} = \frac{1-X^{2n}}{X^{2(n-1)}} = \frac{1-\cos^{2n}\theta}{\cos^{2(n-1)}\theta} \approx \left(\frac{n}{3}\tilde{T}\right)^2. \tag{80}$$

Note that this expression coincides with the first order Hubble expansion approximation given in eq. (73), and thus the slow-roll approximation is an approximation to the attractor solution, since it yields a curve that is tangential to the center manifold in the limit of small $T$. Thus, *apart from the zeroth order approximation, Hubble expansion slow-roll approximations, as well as all slow-roll Hubble expansion based approximants, are approximations for the attractor solution.*

The slow-roll approximation can be generalized by inserting higher order Hubble approximants into $f(y)$. A complication arises since different approximations can be obtained by multiplying expressions by various combinations of $1 \approx X^{2n}f(y)$ (they are all tangential to the center manifolds in the limit of small $T$); we here choose a combination that yields the above slow-roll approximation (which was chosen to coincide with the first order expression in (73)) when setting $f(y) = 1 = g(y)$ below:

$$\begin{aligned}
\Sigma_\dagger &\approx -\frac{n}{3}X^{n-1}\tilde{T}\frac{g(y)}{\sqrt{f(y)}}, \\
g(y) &= f(y) - \frac{y}{n}\frac{df}{dy} \\
&= 1 + \left(1 - \frac{1}{n}\right)y + \left(1 - \frac{2}{n}\right)^2 y^2 + \left(1 - \frac{3}{n}\right)^3 y^3 \\
&\quad + \left(\left(1 - \frac{4}{n}\right)^3 + \frac{2}{n^3}\right)\left(1 - \frac{4}{n}\right)y^4 + \mathcal{O}\left(y^5\right).
\end{aligned} \tag{81}$$

Inserting the rational approximants (76) into (77) leads to the corresponding slow-roll approximants based on the Padé approximants constructed from the Hubble expansion. In Ref. [12] the corresponding curves in the state space **S** on the scalar

field subset $\Omega_m = 0$ are given for $n = 1$ in Fig. 10 and the associated relative errors at the end of inflation at $q = 0$ are given in Table 4. Next we will compare some of the simplest, and thereby the most easily applicable, approximations for each of the above schemes.

## 4.4   Approximant comparisons

As seen from the above discussion, series expansion approximants and slow-roll approximation schemes lead to ambiguities, i.e., different possible types of approximations. This is to be contrasted with the center manifold analysis, which yield a systematic scheme for obtaining a unique sequence of converging approximations for the attractor solution. On the other hand, the strength of slow-roll approximation schemes is that they can be applied to any potential and problem that satisfies the slow-roll conditions; it remains to be seen to what extent this can be accomplished with other methods like center manifold analysis, an issue we will return to elsewhere.

To keep the discussion reasonably short, we here restrict it to comparing only some of the fairly simple approximations, namely: (i) the slow-roll approximation given by $\Sigma_\dagger \approx -\frac{n}{3} X^{n-1} \tilde{T}$, (ii) the center manifold Padé approximant $\theta \approx -\frac{\sqrt{n}}{3} \tilde{T}[1/1]_{f(x)}$ given in eq. (66), which we will refer to as $[1/1]_\theta$, and (iii) the series expansion Padé approximant for $\Sigma_\dagger$ given in eq. (68), which we will refer to as $[1/1]_{\Sigma_\dagger}$. The accuracy of the different approximations for the attractor solution, which is computed numerically, is shown in Figure 4, while the relative errors at $q = 0$ are given in Table 1.[14]

| $n$ | 1 | 2 | 3 | 4 | 5 | 6 | 7 | 8 | 9 | 10 | 15 | 20 |
|---|---|---|---|---|---|---|---|---|---|---|---|---|
| Slow-Roll | 14% | 3% | 19% | 33% | 44% | 54% | 62% | 69% | 75% | 79% | 92% | 97% |
| $[1/1]_\theta$ | 7% | 2% | 6% | 13% | 20% | 27% | 34% | 40% | 45% | 50% | 69% | 81% |
| $[1/1]_{\Sigma_\dagger}$ | 14% | 19% | 22% | 24% | 25% | 26% | 27% | 27.8% | 28.3% | 29% | 30% | 31% |

Table 1: Relative Hubble errors $\frac{|\Delta H|}{H}$ at $q = 0$ for the slow-roll $\Sigma_\dagger \approx -\frac{n}{3} X^{n-1} \tilde{T}$, and the $[1/1]_\theta$ and $[1/1]_{\Sigma_\dagger}$ Padé approximants.

All the presently discussed approximations, including the slow-roll approximation $\Sigma_\dagger \approx -\frac{n}{3} X^{n-1} \tilde{T}$, have quite small errors when $q \approx -1$, which is a reflection of

---

[14]The relative errors are given in terms of the Hubble variable $H$ by $|\Delta H|/H = \frac{|H_{num} - H_{approx}|}{H_{num}} = \left| 1 - \left( \frac{T_{num}(1 - T_{approx})}{T_{approx}(1 - T_{num})} \right)^n \right|$, where the subscript $num$ stands for the numerically computed attractor solution while the subscript $approx$ stands for the approximant.

(a) $n = 2$.
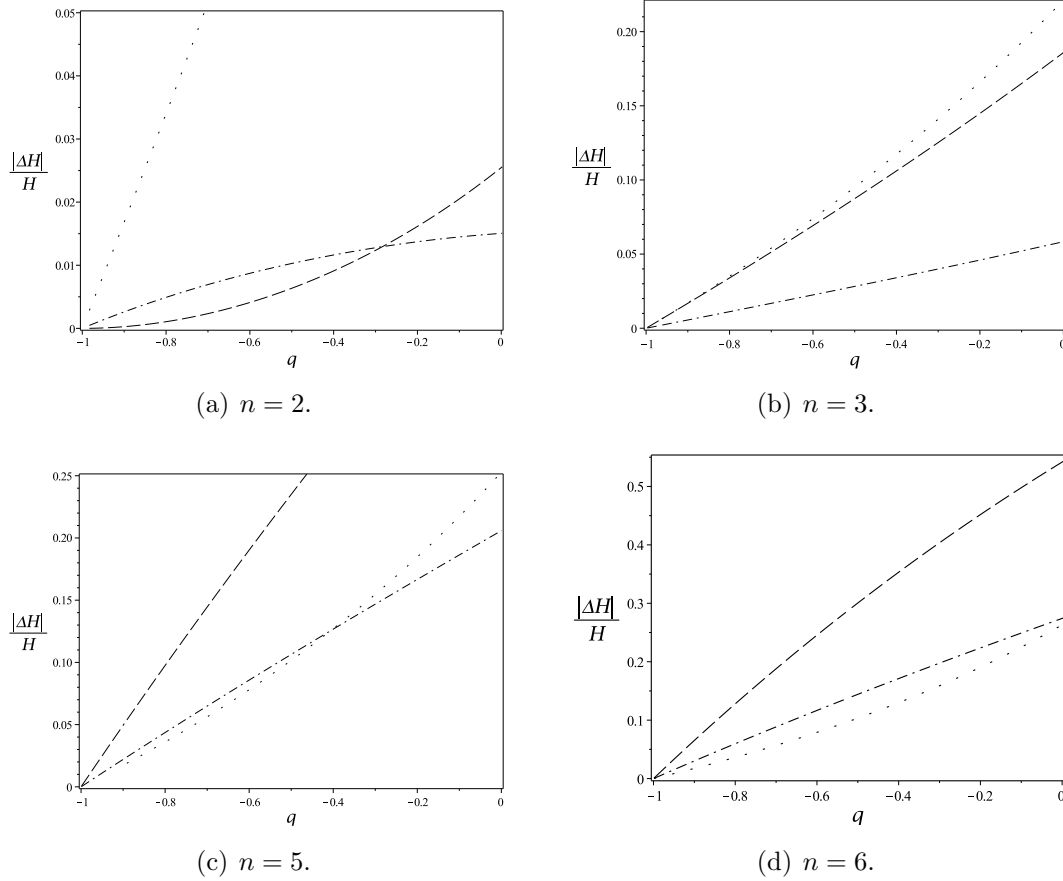


(b) $n = 3$.



(c) $n = 5$.



(d) $n = 6$.

Figure 4: Relative Hubble errors $\frac{|\Delta H|}{H}$ as functions of $q$ for $n = 2, 3, 5, 6$ for the slow-roll approximation (dashed curves), the center manifold Padé approximants $[1/1]_\theta$ (dash-dotted curves), and the $[1/1]_{\Sigma_\dagger}$ Padé approximants (space-dotted curves)

that they are all tangential to the attractor solution when $T \to 0$. For larger $q$ the slow-roll approximation give fairly good results for small $n$ while it becomes less competitive for steep potentials with large $n$ (recall that $\phi \to \pm\infty$ in the de Sitter fixed point limit), as can be expected. However, for small $n$ the slow-roll approximation lead to fluctuations in accuracy when $q$ is no longer close to $-1$, indicating that it sometimes might be rather hard to predict how good the slow-roll approximation actually is going to be in a given situation.

The above suggests that the slow-roll approximation, as well as its more accurate but more complicated higher expansion slow-roll based approximants, should be used with care when it comes to precision cosmology. It should also be pointed out that all approximations get worse for large $n$, hinting at that steep potentials might pose a challenge for approximative methods (although the physical viability of such models might be questioned in view of recent observational data). However, the $[1/1]_{\Sigma_\dagger}$ Padé approximant does not get worse so fast as the other approximations

and for $n \geq 6$ it is the best approximation of the three. This suggests that a good analytic description, pertinent in the context of precision cosmology, might require the development of a variety of complementary approximation methods that can be applied to a range of different problems; we emphasize that the present problem is just an illustrative stepping stone for such developments.

# 5   Concluding remarks

In this paper we have used the inherent physical scales associated with the problem at hand to produce new variables. In particular we obtained a regular dynamical system (7) on a compact state space $\bar{\mathbf{S}}$. This allowed us to give a pictorial description of the entire solution space and moreover give proofs concerning the solutions' asymptotic properties, which in turn were tied to physically important features such as asymptotic manifest self-similarity and breaking thereof. In addition we showed that the so-called attractor solution is just the unstable center manifold of a de Sitter state on the unphysical past boundary subset on $\bar{\mathbf{S}}$. We also found it convenient to introduce several auxiliary dynamical systems, adapted to the physical properties associated with asymptotic past dynamics, since this allowed us to efficiently compute approximations for the attractor solution by means of several complementary approximation schemes. The common feature of these schemes is that to lowest order toward the de Sitter point (apart from those approximations like the lowest order Hubble expansion slow-roll approximation, which just give vertical lines at $q = -1$), from which the attractor solution originate, the approximations yield the tangent space of the center manifold. As a consequence they all lead to that the variable $\tilde{T}$ along the attractor solution in the limit of small $\tilde{T}$ is governed by the approximation

$$\frac{d\tilde{T}}{d\tau} = \frac{n}{3}\,\tilde{T}^3. \tag{82}$$

This, in combination with the definition $\tilde{T} = cH^{-\frac{1}{n}}$ and that $\tau$ can be identified as $\ln a$, yields that when the scale factor $a \to 0$ then

$$H \propto \left[\ln(a_0/a)\right]^{\frac{n}{2}} \to \infty, \tag{83}$$

which is to be contrasted with the exact de Sitter solution for which $H = \text{constant}$.

Finally, we would like to point out that in principle the methods we have introduced have a broader range of applicability than the presently studied models. For example, the use of averaging techniques should be applicable to the dynamics at late times for solutions that approaches a local minimum of a scalar field potential of the form

$$V \propto \phi^{2n}(1 + W(\phi)) \quad \text{where} \quad \lim_{\phi \to 0} W = 0, \tag{84}$$

where we for simplicity have translated the minimum of the potential so that it occurs at $\phi = 0$, and where $W$ obeys suitable differentiability conditions when

$\phi \to 0$. One might question the physical relevance of these potentials at very late times, but it should be pointed out that asymptotic dynamics can be used as pieces to provide approximations for global dynamics, as described in [12].

## Acknowledgments

# References

[1] M. S. Turner. Coherent scalar-field oscillations in an expanding universe. Phys. Rev. **D28** 1243 (1983). DOI: 10.1103/PhysRevD.28.1243.

[2] V. Mukhanov. *Physical foundations of Cosmology*. Cambridge University Press, Cambridge, (2005).

[3] A. D. Rendall. Late-time oscillatory behaviour for self-gravitating scalar fields. Class. Quant. Grav. **24** 667 (2007). DOI: 10.1088/0264-9381/24/3/010.

[4] A. de la Macorra and G. Piccinelli. Cosmological evolution of general scalar fields and quintessence. Phys. Rev. **D61**, 123503 (2000). DOI: 10.1103/PhysRevD.61.123503.

[5] R. Giambo and J. Miritzis. Energy exchange for homogeneous and isotropic universes with a scalar field coupled to matter. Class. Quant. Grav. **27** 095003 (2010). DOI: 10.1088/0264-9381/27/9/095003.

[6] A. A. Coley. *Dynamical systems and cosmology*. Kluwer Academic Publishers, Dordrecht, (2003).

[7] F. Beyer and L. Escobar. Graceful exit from inflation for minimally coupled Bianchi A scalar field models. Class. Quant. Grav. **30** 195020 (2013). DOI: 10.1088/0264-9381/30/19/195020

[8] G. Leon and C. R. Fadragas. Cosmological Dynamical Systems: And their Applications. LAP LAMBERT Academic Publishing (2012).

[9] C. Uggla. Recent developments concerning generic spacelike singularities. Gen. Rel. Grav. **45** 1669 (2013). DOI: 10.1007/s10714-013-1556-3.

[10] M. J. Reyes-Ibarra and L. A. Ureña-López. Attractor dynamics of inflationary monomial potentials. AIP Conference Proceedings **1256**, 293 (2010). DOI: 10.1063/1.3473869.

[11] C. Uggla, R. T. Jantzen, and K. Rosquist. Exact hypersurface homogeneous solutions in cosmology and astrophysics. Phys. Rev. **D51** 5522 (1995). DOI: 10.1103/PhysRevD.51.5522

[12] A. Alho and C. Uggla. Global dynamics and inflationary center manifold and slow-roll approximants. J. Math. Phys. **56** 012502 (2015). DOI: 10.1063/1.4906081

[13] V. A. Belinskiĭ, L. P. Grishchuk, I. M. Khalatnikov and Y. B. Zeldovich. Inflationary stages in cosmological models with a scalar field. Sov. Phys. JETP **62** 195 (1985).

[14] V. V. Kiselev and S. A. Timofeev. Quasiattractor dynamics of $\lambda\phi^4$-inflation. arXiv:0801.2453 (2008).

[15] A. D. Linde. Chaotic inflation. Phys. Let. **B 129** 177 (1983).

[16] J. D. Crawford. Introduction to bifurcation theory. Rev. Mod. Phys. **63** 991 (1991).

[17] J. Wainwright and G. F. R. Ellis. *Dynamical systems in cosmology*. Cambridge University Press, Cambridge, (1997).

[18] A. D. Rendall. Cosmological models and centre manifold theory. Gen. Rel. Grav. **34** 1277 (2002). DOI: 10.1023/A:1019734703162

[19] J. Wainwright, M. J. Hancock and C. Uggla. Asymptotic self-similarity breaking at late times in cosmology. Class. Quant. Grav. **16** 2577 (1999). DOI: 10.1088/0264-9381/16/8/302.

[20] L. Defrise-Carter. Conformal Groups and Conformally Equivalent Isometry Groups. Commun. math. Phys. **40** 273 (1975).

[21] D. M. Eardley. Self-similar Spacetimes: Geometery and Dynamics. Commun. math. Phys. **37** 287 (1974).

[22] G. N. Remmen and S. M. Carroll. Attractor solutions in scalar-field cosmology. Phys. Rev. **D88** (2013). DOI: 10.1103/PhysRevD.88.083518

[23] G. N. Remmen and S. M. Carroll. How many e-folds should we expect from high-scale inflation? Phys. Rev. **D90** (2014). DOI: 10.1103/PhysRevD.90.063517

[24] A. Corichi and D. Sloan. Inflationary Attractors and their Measures. Class. Quant. Grav. **31** 062001 (2014). DOI: 10.1088/0264-9381/31/6/062001

[25] A. R. Liddle, P. Parsons and J. D. Barrow. Formalizing the slow-roll approximation in inflation. Phys. Rev. **D50** 7222 (1994).DOI: 10.1103/PhysRevD.50.7222

[26] J. Carr. *Applications of center manifold theory.* Springer Verlag, New York, 1981.

[27] J. J. Sinou, F. Thouverez and L. Jezequel. Extension of the center manifold approach, using rational fractional approximants, applied to non-linear stability analysis. Nonlinear Dynamics **33** 267 (2003).DOI: 10.1023/A:1026060404109

[28] C. G. Böhmer, N. Chan and R. Lazkoz. Dynamics of dark energy models and centre manifolds. Phys. Lett. B, **714**, 11 (2012). DOI: 10.1016/j.physletb.2012.06.064.

[29] G. A. Baker. *Essentials of Padé Approximants.* Academic Press, New York, (1975).

[30] J. Kallrath. *On Rational Function Techniques and Padé Approximants. An Overview.* (2002).

[31] D. S. Salopek and J. R. Bond. Nonlinear evolution of long-wavelength metric fluctuations in inflationary models. Phys. Rev. **D42** 3936 (1990).

[32] J. A. Sanders, F. Verhulst, J. Murdock *Averaging Methods in Nonlinear Dynamical Systems* Applied Mathematical Sciences 59, Springer (2007).

[33] J. Guckenheimer, P. Holmes. *Nonlinear Oscillations, Dynamical Systems, and Bifurcations of Vector Fields.* Springer, Applied Mathematical Sciences, 42 (2000).

[34] E. A. Coddington, N. Levinson. *Theory of Differential Equations* McGraw-Hill, New Yorck (1955).